Are economists getting climate dynamics right and does it matter?

Simon Dietz[1,2], Frederick van der Ploeg[2,3,4], Armon Rezai[2,5] and Frank Venmans[6,1]

November 10, 2020

Abstract

We show that economic models of climate change produce climate dynamics inconsistent with current climate science models: (i) the delay between CO_2 emissions and warming is much too long and (ii) positive carbon cycle feedbacks are mostly absent. These inconsistencies lead to biased economic policy advice. Controlling for how the economy is represented, different climate models result in significantly different optimal CO_2 emissions. A long delay between emissions and warming leads to optimal carbon prices that are too low and attaches too much importance to the discount rate. Similarly we find that omitting positive carbon cycle feedbacks leads to optimal carbon prices that are too low. We conclude it is important for policy purposes to bring economic models in line with the state of the art in climate science and we make practical suggestions for how to do so.

Keywords: carbon cycle, carbon price, climate change, integrated assessment modelling, positive feedbacks, social cost of carbon

JEL codes: Q54

[1] London School of Economics and Political Science, London, UK

[2] CESifo, Munich, Germany

[3] University of Oxford, Oxford, UK

[4] Vrije Universiteit Amsterdam, Amsterdam, The Netherlands

[5] Vienna University of Economics and Business, Vienna, Austria; IIASA, Laxenburg, Austria

[6] University of Mons, Mons, Belgium

Email for correspondence: s.dietz@lse.ac.uk. We would like to thank the editor and three anonymous referees, as well as David Anthoff, Henk Dijkstra, Carolyn Fischer, Gib Metcalf, Derek Lemoine, Reyer Gerlagh, Thomas Lontzek, Zack Miller, Felix Pretis, Glenn Rudebusch, James Stock and Richard Tol, for their comments and suggestions. We would also like to thank participants at AERE 2020, the Belgian Environmental Economics Day in Hasselt, EAERE 2020, the European Geophysical Union 2020, the LSE-Imperial Workshop in Environmental Economics, and the Virtual Seminar in Climate Economics, as well as seminar participants at Cambridge, CIRED (Paris) and the European University Institute (Florence), for their input. We would like to acknowledge the financial support of the Grantham Foundation and FNRS. SD would also like to thank the Oxford Martin School at the University of Oxford, which hosted him for part of this research. The authors have no conflicts of interest or financial interests to disclose.

1 Introduction

Climate change is arguably the quintessential dynamic problem in economics. Carbon dioxide resides in the atmosphere for centuries after it is emitted, while the climate system operates on timescales ranging from seconds to millennia. Presumably climate dynamics must be accurately represented in economic models of climate change, if appropriate policy prescriptions are to be made. But do economic models get climate dynamics right? To the extent that they don't, does it matter?

This paper aims to make two contributions. First, we highlight some key inconsistencies between how leading economic models of climate change represent climate dynamics and how the current generation of climate science models does. Second, we explore the economic implications of these inconsistencies. Using the economic module of Nobel laureate William Nordhaus' DICE model as a consistent representation of the economy, we quantify how different models of the climate system affect optimal CO_2 prices/taxes, CO_2 emissions and temperatures.

We conduct this study in response to some recent work hinting at a systemic problem. van Vuuren et al. (2011) have documented wide variations in the climate dynamics simulated by a sample of economic models, without analysing the economic implications. Calel and Stainforth (2017) and Rose et al. (2017) have come up with similar findings and also showed that these can result in variations in estimated economic impacts of climate change. In response to Lemoine and Rudik (2017), who argue that inertia in the climate system buys time for optimal CO_2 prices to start low and grow slowly, Mattauch et al. (2020) argue that the Lemoine and Rudik (2017) model is out of line with the temperature impulse response to CO_2 emissions in climate science models, and that bringing it into line significantly alters the optimal CO_2 price path.[1]

We build on these studies in two main ways. First, we attempt a com-

[1]Dietz and Venmans (2019) note a similar discrepancy between DICE 2013 and climate science models, without exploring the direct implications for CO_2 prices.

prehensive assessment of climate dynamics in a representative sample of six leading economic models of climate change, a.k.a. integrated assessment models or IAMs, and we compare them with a canonical set of climate science models. We include not only quantitative IAMs like DICE, but also analytical IAMs built to yield closed-form solutions for optimal CO_2 prices. Second, we demonstrate the implications of different climate dynamics for economic policy by computing optimal paths, using the economic module of DICE to control for all other relevant differences.

In Section 2, we elaborate on how the leading IAMs fail to conform to climate science models. We select six models, which we argue are representative of the climate economics field: the three most influential quantitative IAMs (DICE, FUND and PAGE), together with three analytical IAMs from prominent recent papers (Golosov et al., 2014; Lemoine and Rudik, 2017; Gerlagh and Liski, 2018). We test how their climate modules respond in two experiments, compared with a large sample of 256 counterpart climate science models. The first test is of how fast and how far temperature rises in response to a CO_2 emission impulse. We show that the climate science models uniformly heat up very quickly to a constant, steady-state level, whereas the climate modules of the IAMs heat up much more slowly and do not attain a steady-state temperature within two centuries. The second test is of how removal of atmospheric CO_2 by carbon sinks (i.e. the oceans and biosphere) changes as CO_2 emissions continue. In the climate science models, carbon sinks weaken. Their ability to remove CO_2 from the atmosphere is diminished by positive feedbacks in the carbon cycle, leading to more warming from given emissions. By contrast, we show that CO_2 removal by carbon sinks *strengthens* in most of the IAMs, giving a false impression of increasing absorptive capacity.

Section 3 offers a general framework to understand the models of the carbon cycle and warming process featured in these two experiments, both from climate science and economics. This framework enables us to decompose the dynamic temperature response to a CO_2 emission impulse in the models into the dynamic response of (i) the atmospheric CO_2 concentration and (ii) tem-

perature. This decomposition demonstrates that the IAMs' climate modules vary widely in how fast a CO_2 emission impulse decays and how much is removed from the atmosphere in the long run, and that the decay behaviour generally differs from the representative climate science model. In particular, most of the IAMs remove CO_2 from the atmosphere too slowly at first, which would in fact result in a fast temperature response to a CO_2 emission impulse, all else being equal. The second part of the decomposition shows, however, that almost all of the IAMs exhibit too much temperature inertia in response to elevated atmospheric CO_2. Thus the very slow temperature response to emissions in the IAMs stems from too much temperature inertia.

In Section 4, we move on to exploring the economic implications of different representations of the climate system, i.e. we turn to whether any of this matters for climate policy. We couple various models of the climate system with a common economic module, namely that of DICE. This is sufficient to illustrate in controlled conditions that different climate models result in significantly different optimal CO_2 emissions, concentrations and temperatures, both on emissions paths that maximise social welfare and on emissions paths that minimise CO_2 abatement costs subject to a 2°C warming constraint (per the UN Paris Agreement on Climate Change).

Since the various climate models differ in multiple ways, Section 5 isolates the effects of (i) too long a delay between emissions and warming and (ii) failing to simulate positive carbon cycle feedbacks. On the first, we find a long delay between an emission impulse and warming leads to optimal carbon prices that are too low. It also implies optimal carbon prices are too sensitive to the discount rate, since the costs of global warming are erroneously placed too far in the future. On the second, failing to simulate positive carbon cycle feedbacks also leads to optimal carbon prices that are too low. The effect is larger when cumulative CO_2 uptake and temperature are high and overall it is of comparable size to a long delay. Lastly it is worth noting that we specifically find DICE 2016 heats up too much in the long run and this contributes to the false impression that it is infeasible to limit warming to 2°C as mandated by the UN Paris Agreement.

Section 6 concludes and offers a discussion. Climate dynamics matter. Some other issues in climate economics still matter at least as much, such as how to represent damages. But, unlike damages, the discrepancies between IAMs and current climate science models are easily fixed. We make recommendations on how to do so, depending on the complexity and purpose of those models.

2 Two key tests of climate dynamics

Our first test is of how global mean surface temperature responds to an emission impulse of 100 gigatonnes of carbon in the models. The background atmospheric CO_2 concentration is held constant at 389 parts per million (the level observed in 2010[2]) and the equilibrium climate sensitivity is set to 3.1°C. This replicates a well-known experiment in climate science (Ricke and Caldeira, 2014), which has also been recommended by the US National Academy of Sciences as a key test of the consistency of IAMs with current understanding in climate science (National Academies of Sciences, Engineering, and Medicine, 2017). Appendix A contains further details of the experiment.

To produce this figure, we first compute the temperature impulse response in 256 reduced-form climate science models, which we obtained from the literature.[3] The set of models here corresponds to the so-called CMIP5 ensemble, after the 5th Coupled Model Intercomparison Project of the World Climate Research Programme. We then combine these impulse responses with those of six leading IAMs, including the three most influential quantitative IAMs by far – DICE, FUND and PAGE[4] – and three leading analytical IAMs published

[2]https://data.giss.nasa.gov/modelforce/ghgases/Fig1A.ext.txt

[3]The set of 256 models is the product of all combinations of 16 carbon cycle models and 16 atmosphere-ocean general circulation models (AOGCMs). Many of the underlying models are highly complex and run on super-computers. However, previous research in climate science, which we build on here, shows that the dynamics they simulate for atmospheric CO_2 and global mean surface temperature can be fit with a high degree of precision using reduced-form models (Geoffroy et al., 2013; Joos et al., 2013; Ricke and Caldeira, 2014), which enables comparisons like this one.

[4]We include both DICE 2013 (Nordhaus, 2014) and DICE 2016 (Nordhaus, 2017), due to their divergent behaviour, FUND3.11 (developed by Anthoff and Tol:

in recent years (Golosov et al., 2014; Gerlagh and Liski, 2018; Lemoine and Rudik, 2017). While this sample of economic models is not exhaustive, we argue it is representative of the field as a whole.[5]

Perhaps contrary to popular belief, the temperature response to a CO_2 emission impulse in climate science models is *fast.* Figure 1 shows this. Peaking around ten years after the emission impulse, temperature is then permanently elevated. The response of the models resembles a step function. Dietz and Venmans (2019) explain the underlying geophysics. In comparison, Figure 1 also shows there is far too much delay between the injection of CO_2 and the resulting peak warming in almost all the leading IAMs. The temperature response peaks after 55 years in DICE 2013, 67 years in PAGE and 75 years in the model of Gerlagh and Liski (GL18). In the central case studied by Lemoine and Rudik (LR17) it takes 92 years, in FUND it takes 128 years and in DICE 2016 it takes 180 years. The only model that does not simulate a long delay is that of Golosov et al. (GHKT14), which assumes no delay in the temperature response *a priori.* This turns out to be a reasonable approximation. After peaking, temperature begins to decrease again in the IAMs, which is also contrary to the climate science models.

This experiment involves a fairly large instantaneous emission impulse of 100GtC, which is equivalent to about ten years of CO_2 emissions from burning fossil fuels at current rates (Le Quéré et al., 2018). One may wonder whether the conclusions we draw are robust to the size of the emission impulse. Appendix A shows that they are. Qualitatively very similar results are

https://github.com/fund-model/MimiFUND.jl) and PAGE09 (Hope, 2013).

[5]As an example of their policy application, DICE, FUND and PAGE are used in the United States to estimate the social cost of carbon – the marginal damage cost of CO_2 – for the purposes of cost-benefit analysis of federal regulations (Interagency Working Group on Social Cost of Carbon, 2013). Of the analytical IAMs, the model of Golosov et al. has been particularly widely adopted in subsequent work, with 683 citations according to Google Scholar as of 10 August 2020. Few quantitative or analytical IAMs beyond these have been built to conduct cost-benefit analysis, i.e. to compute welfare-maximising emissions paths under endogenous climate damages/impacts from rising temperatures. The term IAM is sometimes applied to a much wider set of models, including energy models built to assess the costs of meeting pre-defined CO_2 emissions budgets or targets. These models do not have climate modules, however.

Figure 1: Dynamic temperature response of 256 climate science models (the CMIP5 ensemble) and seven IAMs to an instantaneous 100GtC emission impulse against a constant background atmospheric CO_2 concentration of 389ppm. The temperature response of the IAMs is much slower than the climate science models, except Golosov et al. (2014). After 200 years, the temperature response of the IAMs is often well outside the range of the climate science models. The CMIP5 model responses are emulated/fitted by combining the Joos et al. (2013) carbon cycle model and the Geoffroy et al. (2013) warming model.

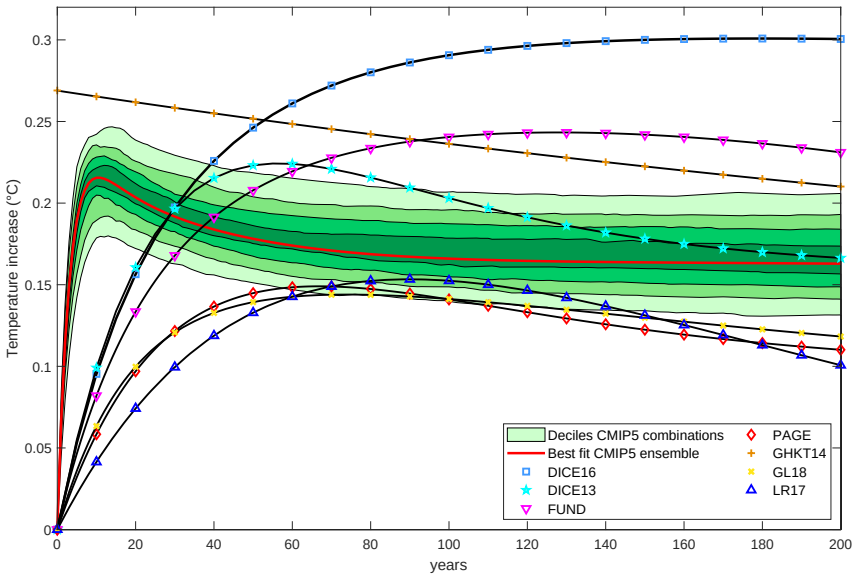

obtained from a much smaller emission impulse (1GtC) and a much larger one (1000GtC). One may also wonder whether the rapid temperature impulse response is consistent with observational data, not just a property of the climate science models (noting these models are themselves calibrated on observations). Montamat and Stock (2020) provide evidence that this is the case, regressing temperature on atmospheric CO_2 using an instrumental variables approach. Lastly, Appendix A also shows that the temperature impulse responses of the models featured in our experiment are qualitatively very similar when background atmospheric CO_2 is rising, rather than being held constant.

In Figure 2, we present the results of our second test. We run the models under a scenario of constant greenhouse gas emissions[6] and plot how yearly uptake of CO_2 by carbon sinks changes as the stock of atmospheric CO_2 increases. Again, a comparison like this was identified by the National Academy of Sciences as a key test of IAMs (National Academies of Sciences, Engineering, and Medicine, 2017). The representative climate science model in this experiment is called FAIR (Millar et al., 2017). FAIR is based on the same reduced-form model used to approximate the climate science models in Figure 1, but adds additional carbon cycle feedbacks. We calibrate FAIR on the mean climate science model depicted in Figure 1, and add carbon cycle feedbacks calibrated on observational data since pre-industrial by Millar et al. (2017). Appendix A contains further details of this experiment.

In FAIR, yearly uptake of CO_2 by carbon sinks decreases as the atmospheric CO_2 concentration increases. Carbon sinks become less effective at removing CO_2 from the atmosphere, because of positive feedbacks in the carbon cycle. In the absence of these feedbacks, yearly uptake of CO_2 by carbon sinks would increase with the atmospheric CO_2 concentration, simply due to Henry's Law.[7] Instead, as atmospheric CO_2 rises, the oceans, like the atmosphere, warm up. As they do so, they keep less CO_2 in solution, so more CO_2 stays in

[6]Fixed at the 2015 level. Doing so enables us to clearly show the effect of carbon cycle feedbacks, which would not be clear on an increasing emissions path, for reasons set out just below.

[7]The amount of dissolved gas in a liquid (i.e. the oceans) is proportional to its partial pressure above the liquid (i.e. in the atmosphere).

Figure 2: Yearly uptake of CO_2 by carbon sinks as a function of atmospheric CO_2 in FAIR and seven IAMs under constant 2015 greenhouse gas emissions. Each marker represents five years. FAIR shows yearly uptake decreases, while the IAMs have it increasing, except FUND.

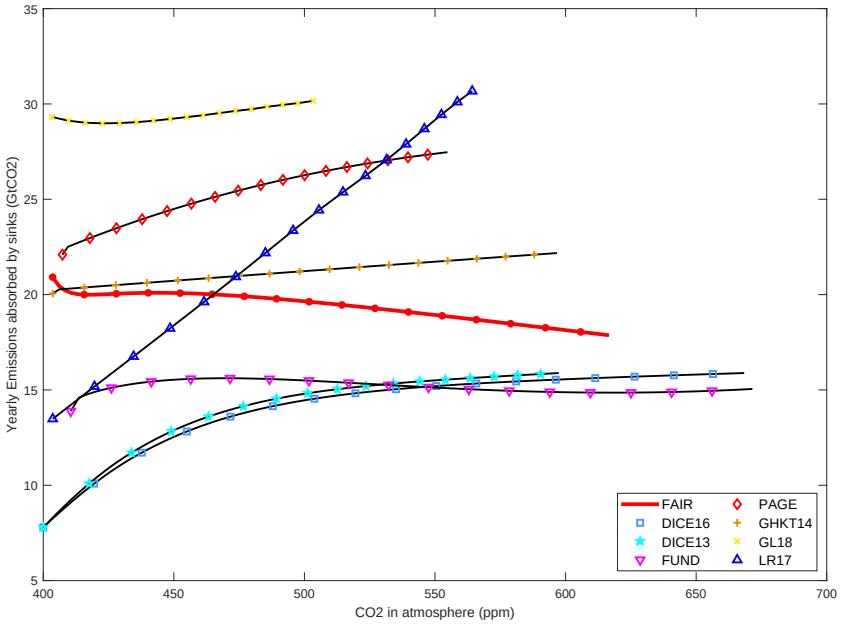

the atmosphere, further increasing temperature. CO_2 reacts with seawater to form carbonic acid, so the more CO_2 the oceans absorb cumulatively, the more acidic they become, which also limits their ability to absorb carbon (Revelle and Suess, 1957). Furthermore, climate change is expected to reduce net uptake of CO_2 by the biosphere.[8] Most of the IAMs do not take these feedbacks into account, however. This explains why in these models there is an *increasing* relationship between atmospheric CO_2 and annual CO_2 removal by carbon sinks. The exceptions are FUND and PAGE, both of which incorporate feedbacks from carbon sinks to atmospheric CO_2/warming. In FUND but not in PAGE, these feedbacks are sufficient to produce a decreasing overall relationship between atmospheric CO_2 and CO_2 removal by sinks.

There is reason to believe these two discrepancies between the current crop of climate science models and the leading IAMs could matter for policy prescriptions. First, given the centrality of discounting in climate economics (Arrow et al., 2013; Gollier, 2012; Nordhaus, 2007; Stern, 2007), the fact that IAMs underestimate warming in the near future in response to a CO_2 emission impulse could significantly impact the welfare evaluation of emissions abatement responses. According to the climate science models, CO_2 emissions elevate temperatures almost immediately. Avoiding those emissions would therefore pay an almost immediate dividend. Second, ignoring the diminishing marginal effectiveness of carbon sinks underestimates the climate response to CO_2 emissions in the long run, which again impacts the welfare evaluation of emissions abatement responses.

[8] Changes to the ocean circulation could also reduce CO_2 uptake (Friedlingstein et al., 2006). Not included here are further positive greenhouse gas feedbacks such as permafrost thawing, which tend instead to be classed as tipping points in the climate system (Lenton et al., 2008).

3 Models of the carbon cycle and temperature dynamics

How do the models used in the previous section – both the climate science models and the IAMs – actually work? In this section, we offer a general framework for understanding this using impulse response functions (see e.g. Maier-Reimer and Hasselmann, 1987). The framework enables us to decompose the temperature response to a CO_2 emission impulse in the models into the response of (i) the atmospheric CO_2 concentration and (ii) temperature. By describing the models in more detail, we also set the scene for our subsequent economic analysis, which is based on coupling different climate models with the DICE economic module.

Start by writing the temperature impulse response to an initial CO_2 emission as plotted in Figure 1 as:

$$\frac{\Delta T_t}{\Delta E_1} = \sum_{s=1}^{t} \frac{\Delta T_t}{\Delta F_s} \frac{\Delta F_s}{\Delta M_s} \frac{\Delta M_s}{\Delta E_1}, \tag{1}$$

where T_t is the increase in global mean temperature at time t relative to pre-industrial, E is CO_2 emissions, F is radiative forcing and M is the atmospheric CO_2 concentration.

The temperature impulse response at time t to a CO_2 emission at time $t = 1$ is thus the sum over the intervening period of the product of the CO_2 concentration impulse response to the emission, $\Delta M_s/\Delta E_1$, the within-period change in forcing in response to atmospheric CO_2, $\Delta F_s/\Delta M_s$, and lastly the change in temperature in response to the additional forcing, $\Delta T_t/\Delta F_s$. The CO_2 concentration impulse response to the emission is determined by a carbon cycle model, while the forcing and temperature response to changing atmospheric CO_2 is determined by a warming model. Let us now scrutinise these two models in turn.

The carbon cycle model

Most simple models of the carbon cycle partition the system into a series of reservoirs or boxes, between which carbon is exchanged. The diffusion of carbon between different boxes (e.g. the atmosphere, biosphere, and upper and lower oceans) can be modelled by a system of difference equations of the form

$$\mathbf{m}_t = \mathbf{A}\mathbf{m}_{t-1} + \mathbf{b}E_t, \tag{2}$$

where the vector $\mathbf{m}_t$ contains the stocks of carbon in each of n boxes at the end of period t and $\mathbf{A}$ is a matrix, whose elements describe the speed of diffusion between the boxes. The vector $\mathbf{b}$ contains the shares of emissions that enter each of the boxes. As the matrix $\mathbf{A}$ and the vector $\mathbf{b}$ are constant, (2) corresponds to a linear carbon cycle.

The atmospheric CO_2 concentration $M_t \equiv \mathbf{d}'\mathbf{m}_t$, where $\mathbf{d}$ is the vector that maps the contents of the various boxes into the stock of atmospheric carbon. Then

$$M_t = \mathbf{d}'\left(\mathbf{A}^t M_0 + \sum_{s=1}^{t} \mathbf{A}^{t-s}\mathbf{b}E_s\right), \tag{3}$$

where M_0 is the initial concentration. In Appendix B, we show how spectral decomposition can be used to obtain the CO_2 concentration impulse response function:

$$\frac{\Delta M_t}{\Delta E_s} = \mathbf{d}'\mathbf{A}^{t-s}\mathbf{b} = \sum_{s=1}^{t}\sum_{i=1}^{n} \psi_i \lambda_i^{t-s}. \tag{4}$$

The $\lambda_i \in (0, 1]$ are the eigenvalues of $\mathbf{A}$, which we assume to be real and in decreasing order of magnitude. These are inversely proportional to how long CO_2 resides in each of the boxes. The constants $\psi_i > 0$ represent the contribution of each box to the atmospheric carbon stock. If a proportion of emissions stays in the atmosphere forever, $\lambda_1 = 1$ for the box pertaining to that proportion ($i = 1$) and the impulse response is the sum of the permanent and transitory components,

$$\frac{\Delta M_t}{\Delta E_s} = \psi_1 + \sum_{i=2}^{n} \psi_i \lambda_i^{t-s}. \tag{5}$$

Equation (5) fully determines any linear carbon cycle model with any number of boxes, which explains why such impulse response functions are commonly used in climate science to represent and compare models of varying degrees of complexity.

Table 1 applies this framework to the carbon cycle models compared in the previous section. Joos et al. (2013) is the representative climate science model, i.e. the model used to fit the CMIP5 ensemble. While the number of boxes varies, most models are based on a structure in which there is a permanent box, into which roughly 1/5 to 1/6 of a CO_2 emission impulse flows, a very slowly decaying box, and one or more boxes that decay much more quickly. However, there is significant variation in both the shares of emissions flowing into each box and the residence time (specifically the half-life) of CO_2 in each of the temporary boxes.[9] Appendix B contains further details of the models' carbon cycles.

What CO_2 dynamics do these different representations give rise to? Figure 3 plots the CO_2 impulse responses of the various models. The impulse size is 100GtC as in the experiments above. The figure shows that the differences between the models' structures and parameters cause significant differences in their CO_2 impulse responses. Some models such as GL18 remove CO_2 very quickly initially. Others such as PAGE remove it very slowly. Over the first 50 years, however, most IAMs remove CO_2 more slowly than the best fit of the CMIP5 ensemble, which in itself would tend to produce a *fast* temperature impulse response. After a couple of centuries, some IAMs such as LR17 remove most of the CO_2 emission impulse. Others such as DICE 2016 and FUND remove relatively little. By then, there does not appear to be a systematic bias between the IAMs and the best fit of CMIP5. Overall, few of the IAMs resemble the best fit of CMIP5, however.

So far we have not addressed weakening carbon sinks. It is clear these are not represented by linear models, since the CO_2 impulse response in Equation

[9]The shares flowing into the three boxes of the GL18 model do not add up to one, since only 94% of box 1 pertains to the atmosphere (the rest is assumed to be absorbed immediately by the upper ocean). The half-life of CO_2 in box 2 of DICE 2016 is much larger than in earlier versions of DICE, or in the other models shown.

Table 1: Comparing key linear carbon cycle models

Model	Time step (years)	Box 1. Permanent	2. Temporary	3. Temporary	4. Temporary	5. Temporary
DICE 2016	5	22%	41%; 851 years	37%; 9 years		
DICE 2013	5	5%	26%; 1675 years	69%; 26 years		
FUND	1	13%	20%; 252 years	32%; 51 years	25%; 12 years	10%; 1.4 years
PAGE	varies	19%	43%; 73 years	38%; <1 years		
GHKT14	10	20%	31%; 300 years	49%; <10 years		
GL18	10	16%	18%; 91 years	44%; 11 years		
LR17	1		100%; 50 years			
Joos et al. (2013) / best fit CMIP5 ensemble	1	22%	22%; 277 years	28%; 25 years	28%; 3 years	

Key: the first figure in each cell is the contribution of box i to the atmospheric carbon stock (ψ_i) and the second figure the time it takes for half of the carbon to have left box i ($\ln(0.5)/\lambda_i$ for the continuous time model of Joos et al. (2013) and timestep $\times \ln(0.5)/\ln(\lambda_i)$ for the other models, which are in discrete time). Both FUND and PAGE include additional positive carbon cycle feedbacks that are not included in this table.

Figure 3: Removal of a 100GtC emission impulse (47ppm CO_2) in climate science models and seven IAMs against a constant background atmospheric CO_2 concentration of 389ppm. There are big differences between the IAMs. Few of the IAMs approximate the best fit of the climate science model distribution. Note that FAIR removes less CO_2 from the atmosphere against a higher background concentration due to positive carbon cycle feedbacks.

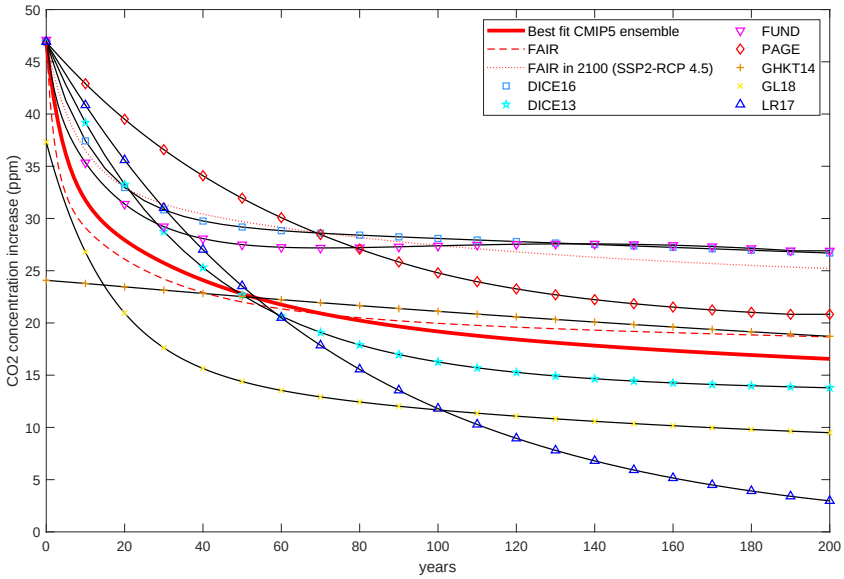

(4) does not depend on cumulative absorbed carbon, or temperature. Simple non-linear models of carbon cycle feedbacks include NICCS (Hooss et al., 2001) and FAIR (Millar et al., 2017). FAIR, which is now widely used, simulates weakening carbon sinks by extending the four-box carbon cycle of Joos et al. (2013). Relegating the details to Appendix A, in essence FAIR works by reducing the rate at which carbon is removed from the atmosphere using a scaling factor α (i.e. replace the λ_i with λ_i/α), which is increasing in cumulative carbon uptake and temperature. Figure 3 shows FAIR's positive carbon cycle feedbacks in action: less CO_2 is removed from the atmosphere when the emission impulse is against a higher (year 2100) background concentration of CO_2.[10]

Radiative forcing and temperature dynamics

The relationship between atmospheric CO_2 and forcing is logarithmic, since CO_2 becomes less effective at absorbing outgoing radiation at higher concentrations. The change in forcing in response to atmospheric CO_2 can be written as

$$\frac{\Delta F_s}{\Delta M_s} = \frac{F_{2\times CO_2}}{\ln 2}\frac{1}{M_s}, \tag{6}$$

where $F_{2\times CO_2}$ is the radiative forcing resulting from doubling atmospheric CO_2. This partly determines the equilibrium climate sensitivity, which we hold constant across all the models in order to isolate the effect of short- and medium-run dynamics (see Appendix B). It is important to bear in mind that *total* radiative forcing is the sum of forcing from CO_2 and from other greenhouse gases and forcing agents. Typically these other gases/forcing agents are exogenous in the models,[11] but their role is not trivial[12] and must be properly accounted for. Below we show that failing to do so in some models gives

[10]Corresponding with the year 2100 on the IPCC's RCP4.5 scenario. RCP stands for Representative Concentration Pathway. IPCC developed four RCP scenarios for the *Fifth Assessment Report* (Moss et al., 2010).

[11]In FUND and PAGE, some of the other greenhouse gases, such as methane and nitrous oxide, are explicitly modelled.

[12]The contribution to total radiative forcing of gases/drivers other than CO_2 is about 25% currently (IPCC, 2013).

misleading results.

Just like carbon cycle models, simple warming models typically partition the system into boxes, between which heat is exchanged (e.g. the atmosphere/upper ocean and deep ocean). Thus we can again use spectral decomposition to obtain an analogous expression for the temperature response to forcing:

$$\frac{\Delta T_t}{\Delta F_s} = \sum_{s=1}^{t} \sum_{i=1}^{2} \psi_i^T \lambda_i^{T\, t-s}, \tag{7}$$

where ψ_i^T and λ_i^T denote respectively the shares/weights and eigenvalues of the heat boxes (the superscript T just indicates that these apply to temperature).

Table 2 summarises the dynamics of the various warming models that map forcing into temperature. Geoffroy et al. (2013) is the representative climate science model used to fit the CMIP5 ensemble. Both DICE and Geoffroy et al. (2013) have two boxes representing the temperature of the atmosphere/upper oceans and the deep oceans respectively. However, critically DICE displays a much more sluggish response of temperature to radiative forcing than Geoffroy et al. (2013), especially as the fast box of Geoffroy et al. has a half-life of only 3 years.

Figure 4 uses Equations (6) and (7) to plot the dynamic temperature response of the models to a *constant* increase in atmospheric CO_2 of 100GtC (47ppm). This is therefore the second element of the decomposition of the temperature response to an emission impulse. With the exception of GHKT14, all of the IAMs exhibit a more sluggish temperature response than the best fit of the CMIP5 ensemble. The temperature response of LR17 is particularly slow. After 200 years, temperature is higher in DICE 2013, DICE 2016 and FUND, while LR17 and PAGE are close to the best fit of the CMIP5 ensemble at that moment. The GHKT14 model shows an immediate, permanent increase in temperature. It over-predicts temperature compared with the best fit of the CMIP5 ensemble.

Table 2: Comparing linear temperature-forcing responses

	Time step (years)	Box 1	Box 2
DICE 2016	5	9.9%; 25 years	0.2%; 150 years
DICE 2013	5	9.9%; 23 years	0.2%; 148 years
FUND	1	100%; 31 years	
PAGE	varies	100%; 24 years	
GHKT14	10	n.a.	n.a.
GL18	10	100%; 34 years	
LR17	1	100%; 50 years	
Geoffroy et al. (2013) / best fit CMIP5 ensemble	1	13.5%; 3 years	0.2%; 167 years

Key: The first figure in each cell is the weight of each mode and the second figure the half-life for each mode. PAGE models regional temperature and calculates global temperature as the area-weighted average. GHKT14 effectively assume that temperature is driven by equilibrium climate sensitivity according to Arrhenius' law and do not have any lag between forcing and temperature.

Figure 4: Dynamic temperature response of the best-fit climate model and seven IAMs to a constant increase in atmospheric CO_2 of 100 GtC (47ppm CO_2). The IAMs respond much more slowly to elevated CO_2 than the best-fit climate model, except GHKT14.

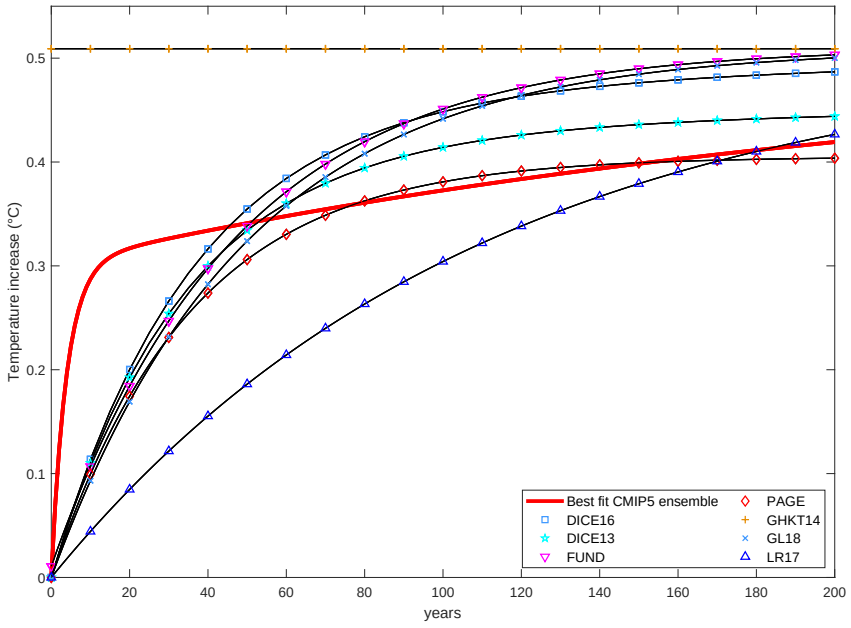

Going back to Figure 1, the IAMs (excluding GHKT14) warm up too slowly in response to the emission impulse. This impulse response is obtained by convoluting atmospheric CO_2 decay/removal as plotted in Figure 3 with temperature inertia as plotted in Figure 4. Thus the analysis of this section shows that the sluggish temperature response to the emission impulse is due to too much temperature inertia in response to elevated atmospheric CO_2. If anything, the IAMs have too little CO_2 decay, but this does not compensate for the inertia. In the best fit of the CMIP5 ensemble, temperature inertia almost exactly offsets CO_2 decay. As a result, the CMIP5 temperature response resembles a step function.

4 Economic policies with different climate models

In this and the following section, we evaluate what difference the model of the climate system makes for economic policies. We focus on two such policies: (i) optimal emissions that maximise social welfare and (ii) a representative policy run in the context of the United Nations climate framework that limits warming to 2°C at minimum discounted abatement cost. The latter path is sometimes described as an exercise in cost-effectiveness analysis (as opposed to (i), which is an exercise in cost-*benefit* analysis) and is a core use of IAMs by IPCC (see Clarke et al., 2014).[13]

To perform this evaluation, we need to make a controlled comparison, in which the models are identical in all respects except how they represent the dynamics of the carbon cycle and warming process. Control is achieved by using the DICE 2016 economic and welfare modules as a common base, and coupling it with different models of the climate system (Table 3).[14] We

[13] Abatement cost minimisation subject to a temperature constraint is the same as welfare maximisation subject to a temperature constraint and ignoring climate damages.

[14] Readers are referred to William Nordhaus' web resources for a comprehensive description of the DICE 2016 economic module and, unless otherwise specified, the version we use is unchanged. See https://sites.google.com/site/williamdnordhaus/dice-rice.

drop the FUND and PAGE models here, due to the practical difficulties of coupling these more complex IAMs with the DICE 2016 economy. Note that temperature is only implicit in GHKT14 and GL18, however it can be backed out using assumptions explicitly stated in these papers.

Table 3: List and description of models used for economic evaluation

Model	Description
DICE 2016	Standard DICE 2016 economy and climate
DICE-DICE 2013	DICE 2016 economy with the DICE 2013 climate module
DICE-GHKT14	DICE 2016 economy with the Golosov et al. (2014) climate module
DICE-GL18	DICE 2016 economy with the Gerlagh and Liski (2018) climate module
DICE-LR17	DICE 2016 economy with the Lemoine and Rudik (2017) climate module
DICE-FAIR-Geoffroy	DICE 2016 economy with the FAIR carbon cycle and the Geoffroy et al. (2013) warming model
DICE-Joos-Geoffroy	DICE 2016 economy with the Joos et al. (2013) carbon cycle and the Geoffroy et al. (2013) warming model

Figure 5 plots welfare-maximising carbon prices, emissions and temperatures (left column) from DICE 2016, DICE-FAIR-Geoffroy (i.e. the representative or benchmark climate science model, coupled with the DICE economy), DICE-DICE 2013, DICE-GHKT14, DICE-GL18 and DICE-LR17. It is immediately apparent that the models differ significantly in their welfare-maximising paths. Initial carbon prices range from \$11/tCO_2 in DICE-LR17 to \$57 in DICE-GHKT14, with an initial carbon price of \$30 in the benchmark DICE-FAIR-Geoffroy model, and \$37 in standard DICE 2016. These differences grow over time, such that by 2100 the range is \$77-358/tCO_2.

Welfare-maximising CO_2 emissions and temperatures also vary widely. Initial CO_2 emissions range from 33GtCO_2 in DICE-GHKT14 to 40GtCO_2 in DICE-LR17, while in 2100 they range from nearly zero to 50GtCO_2. Optimal warming by the end of the century ranges from just 2.0°C in DICE-LR17 to 4.0°C in DICE-GHKT14. Optimal warming in the benchmark DICE-FAIR-Geoffroy model is 3.0°C in 2100. Notice that optimal warming in 2100 is

lowest in DICE-LR17, despite this model having the lowest carbon prices and the highest emissions. This is directly attributable to its slow and low temperature impulse response to CO_2 emissions, as shown in Figure 1. Notice also the high initial starting temperature in DICE-GHKT14. Temperature is only implicit in GHKT14, but can be backed out from their assumptions about the atmospheric carbon stock and damages. Their assumption of no delay between emissions and warming, coupled with a calibration that ignored the contribution of non-CO_2 greenhouse gases to warming, leads to this artefactual result.

Figure 5 also compares models on a path that limits warming to 2°C at minimum discounted abatement cost (right column). Similar to the models' welfare-maximising paths, we observe large differences in their 2°C cost-minimising paths. Naturally, given the warming constraint, the differences are particularly evident in carbon prices and emissions. Initial carbon prices vary from \$13/tCO_2 in DICE-LR17 to \$143 in standard DICE 2016. By mid-century the range of carbon prices peaks at \$406/tCO_2 between these models. Initial CO_2 emissions range from 26GtCO_2 in DICE 2016 to 40GtCO_2 in DICE-LR17. Limiting warming to 2°C is infeasible in DICE-GHKT14, for the reasons mentioned above. In order to limit warming to 2°C, emissions must eventually be negative in all models, but the time at which 'net zero' is crossed ranges from just before 2050 in DICE 2016 to just after 2100 in DICE-LR17. Although warming is limited to 2°C, the temperature trajectory shows significant variation across the models, particularly in mid-century. The range is 1.2-1.8°C in 2050, for instance. Note these 2°C cost-minimising paths are obtained assuming CO_2 emissions from land-use change and forestry, as well as radiative forcing from other greenhouse gases and atmospheric agents, follow the IPCC RCP2.6 scenario, which is the only RCP scenario consistent with the 2°C target. We will return to this point below.

Figure 5: Welfare-maximising (left) and cost-minimising (right) paths from different climate models coupled with the DICE 2016 economy. Top row – carbon prices; middle row – CO_2 emissions; bottom row – warming. The models produce very different carbon price paths, resulting in very different CO_2 emissions and temperature paths.

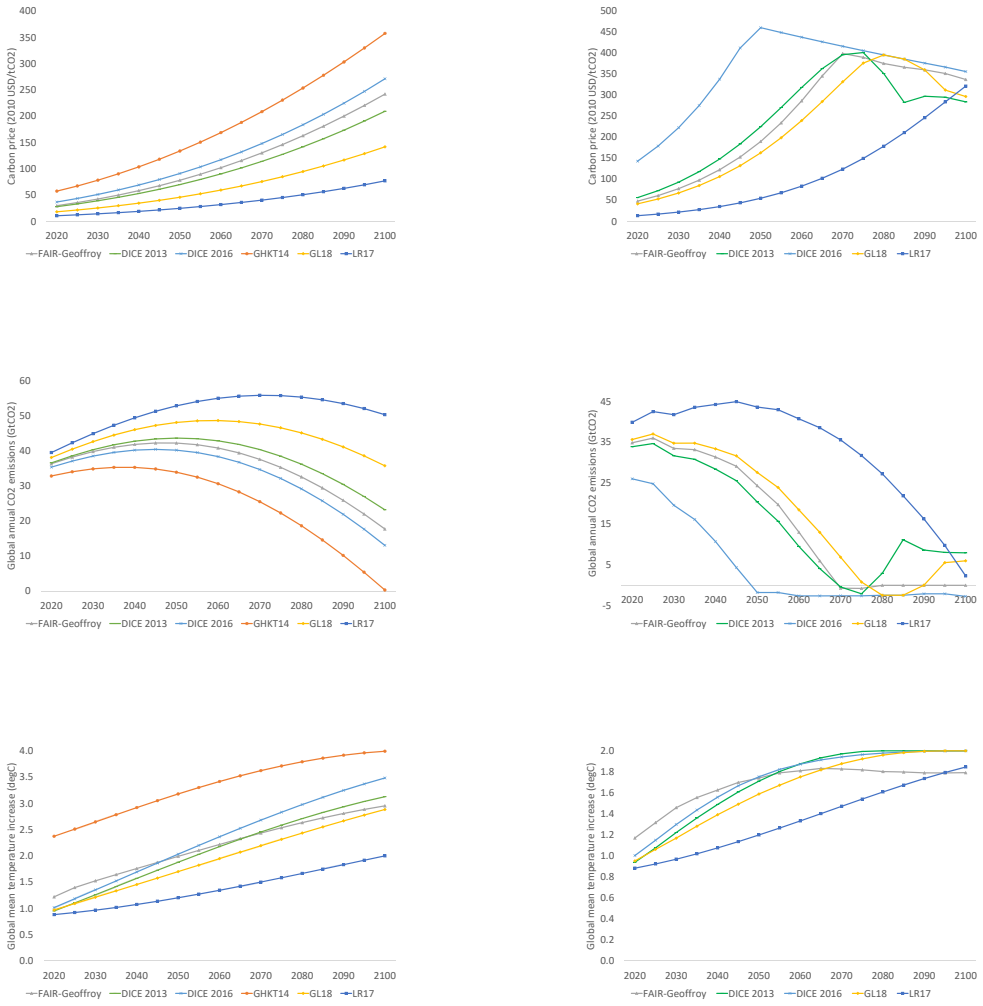

5 Warming delay, positive carbon cycle feedbacks and further economic analysis

While Figure 5 illustrates that climate dynamics matter for economic policies, it does not fully illuminate the role of the issues identified in Section 2, namely

the excessive delay between a CO_2 emission impulse and warming, and the omission of positive feedbacks in the carbon cycle. That is because the climate modules considered differ in multiple respects. Therefore these two issues are explored further in Tables 4 and 5.

To isolate the effect of excessive delay between a CO_2 emission impulse and warming, we construct two further artefact models, built on the DICE-Joos-Geoffroy model used to represent the CMIP5 models in Figure 1. These two models exhibit the same long-run temperature response to a CO_2 emission impulse as DICE-Joos-Geoffroy, but reach that long-run response at very different speeds; far too slowly in comparison with the climate science models, more in line with the IAMs. The reason we construct these two further models is that, even with the same equilibrium climate sensitivity, the different climate models compared above exhibit not only different short- and medium-run temperature dynamics, they also exhibit different long-run temperature responses (as is clear from Figure 1). The new 'Delay 56' model is so called, because it exhibits a delay between the CO_2 emission impulse and peak warming that is five times longer than DICE-Joos-Geoffroy (56 years, rather than 11.2 years). The 'Delay 112' model exhibits a corresponding warming delay that is ten times longer. Appendix B provides further details of these new models.

Table 4 shows that on the welfare-maximising path an excessive delay leads to lower carbon prices throughout. The 2020 carbon price falls from \$27/tCO_2 for the short delay (DICE-Joos-Geoffroy) to \$23 for the 56-year delay and \$18 for the 112-year delay (compare rows 2-4). These differences grow over the course of the century. By 2100, moving from a 10-year delay to a 112-year delay reduces the optimal carbon price by \$75, or 38%. With lower carbon prices naturally come higher CO_2 emissions, but not higher temperatures, since a longer delay means that it takes much longer for the warming effect of these additional emissions to be realised. Table 5 shows that on the 2°C cost-minimising path an excessive delay leads to lower carbon prices in 2020 and 2050. The effect is somewhat smaller than on the optimal path, since the temperature constraint binds and leaves less room for manoeuvre. Lower

carbon prices again result in higher emissions, but the delay means this does not translate into higher temperatures; on the contrary.

An implication of these results is that the optimal path may be less sensitive to assumptions about the discount rate than previously thought. Table 6 shows this is indeed the case. We ran DICE-Joos-Geoffroy and the Delay 56 and 112 variants under standard DICE assumptions about the social discount rate (a pure rate of time preference of 1.5% and an elasticity of marginal utility of consumption of 1.45), and assuming the social planner uses lower values (PRTP=0.1%; elasticity of marginal utility of 1). We call the latter 'public' discounting.[15] The parameter values are the same as in the *Stern Review* (Stern, 2007). With a representative initial growth rate of global mean consumption per capita of 2.5%, the standard DICE discount rate is 5.1% while the 'public' discount rate applied to climate policy is 3.5%. Table 6 shows that the increase in the 2020 optimal carbon price brought about by switching from standard to public discounting is 68% in Delay 112, but only 50% in DICE-Joos-Geoffroy with the short delay. In 2100 the increases are 51% and 38% respectively.

To isolate how positive carbon cycle feedbacks affect model paths, we now compare DICE-FAIR-Geoffroy and DICE-Joos-Geoffroy (rows 1 and 2). DICE-FAIR-Geoffroy includes such feedbacks, while DICE-Joos-Geoffroy does not. These two models are otherwise identical. Introducing the positive carbon cycle feedbacks results in a higher optimal carbon price. In 2020, the optimal carbon price in DICE-FAIR-Geoffroy is \$29.68/tCO_2, \$2.70 above the optimal carbon price in DICE-Joos-Geoffroy. Hence the effect is not quantitatively large in the short run. However, it is in the nature of the carbon cycle feedbacks that they have a larger effect, the higher is cumulative absorbed carbon, and temperature, so we see the gap between the models' optimal carbon prices widening steadily until by 2100 it is \$83/tCO_2. Higher optimal carbon prices result in lower emissions in DICE-FAIR-Geoffroy and this in turn results in

[15]We assume private agents keep the standard DICE parameters for investment/consumption decisions, but that the social planner sets carbon prices using the lower rate (van der Ploeg and Rezai, 2019).

Table 4: Welfare-maximising paths with variants of the DICE model. Comparing DICE-Joos-Geoffroy to Delay 56 and Delay 112 shows that an excessive warming delay results in lower carbon prices, higher CO_2 emissions, but lower temperatures. Comparing DICE-FAIR-Geoffroy (with positive carbon cycle feedbacks) to DICE-Joos-Geoffroy (no feedbacks) shows that positive feedbacks result in higher carbon prices, particularly in the long run, lower emissions and temperatures.

				2020	2050	2100	2020	2050	2100	2020	2050	2100
	Model	Carbon-cycle feedback	Temp. model	Carbon price (USD/tCO_2)			CO_2 emissions ($GtCO_2$)			Warming (°C)		
1	DICE-FAIR-Geoffroy	Yes	Short delay	29.68	78.17	242.18	36.37	42.28	17.75	1.22	1.99	2.95
2	DICE-Joos-Geoffroy	No	Short delay	26.97	66.53	197.61	36.76	44.23	25.28	1.25	2.08	3.01
3	Delay 56	No	Long delay	23.02	55.45	159.01	37.35	46.28	32.38	0.98	1.81	2.93
4	Delay 112	No	Long delay	17.88	42.17	122.98	38.19	48.91	39.68	0.92	1.52	2.67
5	DICE 2016	No	Long delay + too hot later	36.72	91.04	271.34	35.40	40.25	13.07	1.02	2.03	3.48

Table 5: 2°C cost-minimising paths in variants of the DICE model. Comparing DICE-Joos-Geoffroy to Delay 56 and Delay 112 shows that an excessive warming delay results in lower carbon prices and higher emissions in 2020 and 2050, but lower temperatures. Comparing DICE-FAIR-Geoffroy (with positive carbon cycle feedbacks) to DICE-Joos-Geoffroy (no feedbacks) shows that positive feedbacks result in higher carbon prices in 2020 and 2050, lower emissions and temperatures.

				2020	2050	2100	2020	2050	2100	2020	2050	2100
	Model	Carbon-cycle feedback	Temp. model	Carbon price (USD/tCO_2)			CO_2 emissions ($GtCO_2$)			Warming (°C)		
1	DICE-FAIR-Geoffroy	Yes	Short delay	47.98	189.91	337.33	34.88	24.38	0.00	1.17	1.74	1.79
2	DICE-Joos-Geoffroy	No	Short delay	41.62	167.56	337.34	35.65	27.05	0.00	1.20	1.84	1.89
3	Delay 56	No	Long delay	39.41	159.58	318.24	35.93	28.03	2.79	0.97	1.66	2.00
4	Delay 112	No	Long delay	35.83	140.72	357.64	36.40	30.44	-2.79	0.91	1.43	1.96
5	DICE 2016	No	Long delay + too hot later	142.95	460.68	356.31	26.05	-1.76	-2.71	1.00	1.67	2.00

Table 6: Sensitivity of optimal carbon prices to the discount rate. The longer is the warming delay, the more sensitive optimal carbon prices are to a change in the discount rate.

Model	Discount	2020	2030	2040	2050	2060	2070	2080	2090	2100
DICE-Joos-Geoffroy	Standard	26.97	37.55	50.64	66.53	85.52	107.86	133.86	163.72	197.61
	Public	40.45	53.20	71.53	94.24	121.13	152.31	187.95	228.20	273.12
	% diff.	**50.0**	**41.7**	**41.3**	**41.6**	**41.6**	**41.2**	**40.4**	**39.4**	**38.2**
Delay 56	Standard	23.02	31.79	42.54	55.45	70.73	88.55	109.12	132.57	159.01
	Public	36.59	47.44	63.25	82.70	105.50	131.68	161.29	194.30	230.49
	% diff.	**59.0**	**49.2**	**48.7**	**49.1**	**49.2**	**48.7**	**47.8**	**46.6**	**44.9**
Delay 112	Standard	17.88	24.38	32.41	42.17	53.82	67.56	83.57	102.00	122.98
	Public	30.07	38.09	50.46	65.93	84.25	105.41	129.46	156.41	186.10
	% diff.	**68.2**	**56.3**	**55.7**	**56.4**	**56.5**	**56.0**	**54.9**	**53.3**	**51.3**

lower 21st-century warming.[16] Reduced CO_2 uptake by carbon sinks reduces the cumulative emissions budget for limiting warming to 2°C in DICE-FAIR-Geoffroy, so the 2°C cost-minimising carbon price is also higher, resulting in lower emissions and, at least in this century, lower temperatures.

We complete this section with further analysis of two issues. Firstly, Tables 4 and 5 show that DICE 2016 yields higher carbon prices than the benchmark climate science model, DICE-FAIR-Geoffroy (compare rows 1 and 5), particularly on a 2°C cost-minimising path. This leads to lower emissions in DICE 2016, yet temperatures end up being higher. Appendix C provides some further analysis of what is behind the difference between standard DICE 2016 and DICE-FAIR-Geoffroy. Three factors are at play, namely differences in (a) temperature dynamics, (b) removal of atmospheric CO_2 (under constant background atmospheric CO_2) and (c) assumptions about positive carbon cycle feedbacks. In Appendix C, we apportion the difference between (a)-(c) and find that the main driver of different temperatures is (a) the tendency of DICE 2016 to heat up too much in the long run.

Secondly, previous work with DICE 2016 found it is infeasible to limit warming to 2°C (Nordhaus, 2017).[17] Our analysis suggests this is not the case if (a) an appropriate assumption is made about contributions to radiative forcing beyond energy/industrial CO_2 and (b) the climate system is appropriately responsive to CO_2 emissions. In our 2°C cost-minimising runs, we substitute standard DICE 2016 exogenous emissions of CO_2 from land-use change and forestry with corresponding emissions from the IPCC's RCP2.6 scenario[18], which are lower and more consistent with limiting warming to 2°C. We do the same for exogenous radiative forcing from other greenhouse gases and atmospheric agents. This explains why we find it is feasible to limit warming to 2°C in DICE 2016. However, Figure 5 and Table 5 show that, while it is feasible in

[16] Warming is higher in DICE-FAIR-Geoffroy in the longer run, due to the carbon cycle feedbacks' continuing effect. The crossing point is 2200 (not shown). In steady state, optimal warming in DICE-FAIR-Geoffroy is exactly 3°C, while in DICE-Joos-Geoffroy it peaks at about 2.83°C.

[17] Under the constraint of no negative emissions technology in the first several decades.

[18] Specifically when combined with the SSP1 socio-economic scenario; see Moss et al. (2010).

DICE 2016, it is still very expensive. It is much less expensive in DICE-FAIR-Geoffroy, due to its more immediate and ultimately lower temperature impulse response to CO_2 emissions. Appendix C provides some further analysis of this issue too.

6 Conclusions and discussion

We have investigated atmospheric carbon and temperature dynamics in climate models from both climate science and economics. Closely following experimental protocols developed in climate science, we have used reduced-form impulse response functions built to emulate the behaviour of an ensemble of highly non-linear and large-scale Earth System models, and we have compared these with a representative sample of IAMs from the economic literature. We have not been concerned with fitting our reduced-form models to historical data. This would have been a different exercise and the resulting model would be of limited relevance for the analysis of climate policy today. A model calibrated on historical conditions and designed to reproduce the behaviour of past climates is not a reliable model of the future climate. One important reason why is that positive feedbacks in the uptake of atmospheric carbon, studied in some depth in this paper, kick in more strongly when cumulative carbon uptake and temperature are already high (e.g. Millar et al., 2017). This partly explains why climate scientists tend to use the dynamic behaviour of Earth System models in simulation experiments in contemporary and future climatic conditions as their benchmark when building reduced-form models, not past, observed changes in atmospheric carbon and temperature.[19]

There is wide variation in how IAMs simulate the evolution of atmospheric carbon and temperature, but almost all of them are unified in one feature: they show too sluggish a temperature response to an impulse change in CO_2

[19]That being said, Millar et al. (2017) show that the FAIR model, with its flexible representation of positive carbon cycle feedbacks, closely tracks observed global mean temperature when run with estimated historical greenhouse gas emissions. In addition, Montamat and Stock (2020) provide supporting evidence of the fast temperature impulse response to CO_2 emissions, taking an econometric approach to observational data.

emissions compared with the climate science models. This sluggish temperature response in the IAMs is primarily due to too much temperature inertia in response to elevated atmospheric CO_2, rather than CO_2 decaying too quickly (on the contrary, in most IAMs it decays too slowly). Besides the sluggish temperature response to CO_2 emissions, we have also scrutinised the treatment of carbon sinks in the models. In climate science models, carbon sinks weaken due to positive carbon cycle feedbacks. Most IAMs do not demonstrate this property, however.

These discrepancies can cause IAMs to yield misleading policy implications. Controlling for the specification of the economy and welfare using the DICE 2016 economic module, we have found IAMs' climate modules deliver carbon prices, emissions and temperature paths that vary widely and that differ from the benchmark model in climate science. We explored both welfare-maximising carbon prices and carbon prices that ensure a 2°C temperature target is achieved at minimum discounted abatement cost. Some models deliver carbon prices that are higher than the benchmark model, some lower. Further exploring the causes of these differences, we found that a sluggish temperature response to CO_2 emissions – excessive delay – leads to carbon prices that are too low and that are too sensitive to the choice of discount rate, since the costs of global warming are erroneously placed too far in the future. We also found that failing to account for positive carbon cycle feedbacks leads to carbon prices that are too low, especially when atmospheric CO_2 is high. But even if the temperature response to CO_2 emissions is too slow and positive carbon cycle feedbacks are omitted, carbon prices can still be too high in IAMs, as appears to be the case in DICE 2016, which has too high a long-run temperature response.

Therefore climate dynamics matter for economic policy prescriptions. We do not claim they matter more than other *causes célèbres* in climate economics like the social discount rate or the damage function, but matter they do. Moreover, in contrast to these other issues, on which research is ongoing but seemingly far from a definitive conclusion, the discrepancies we have identified between economic models and climate science models can easily be fixed.

We can readily identify two options. The first is to recalibrate or replace the climate modules in IAMs. Models of the carbon cycle need to incorporate positive feedback effects, as FAIR does (Millar et al., 2017). Models of temperature dynamics need to either be replaced or recalibrated, so that they can reproduce the fast temperature response of Earth System models to CO_2 emissions, as the model of Geoffroy et al. (2013) does. Recall the Geoffroy et al. model is structurally identical to the DICE climate module, so DICE would simply need to be recalibrated. Appendix D provides GAMS code to implement the FAIR-Geoffroy climate in DICE. Other simple models in climate science may do the same job. None of these changes requires significant complication of existing IAMs.

The second option is simply to specify temperature as a linear function of cumulative CO_2 emissions (Collins et al., 2013). This is an indirect solution to the problem, because it turns out that the step temperature impulse response function and positive carbon cycle feedbacks combine to produce this linear response in terms of cumulative CO_2 emissions (Dietz and Venmans, 2019).[20] Appendix E demonstrates this: the CMIP5 models exhibit an approximately linear warming response to cumulative emissions under various IPCC emissions scenarios. The IAMs tend not to. The CMIP5 ensemble gives multi-model mean temperature at time t as 1°C plus 1.7°C per trillion tons of cumulative emissions (TtC) from 2020 onwards. Warming from non-CO_2 greenhouse gases needs to be added on top. The slope coefficient of 1.7°C/TtC is known as the Transient Climate Response to Cumulative Carbon Emissions (TCRE).[21] As

[20]Some recent studies that have used this simple relationship to derive economically optimal climate policies are Allen (2016), Brock and Xepapadeas (2017), van der Ploeg (2018), Manoussi et al. (2018) and Dietz and Venmans (2019).

[21]The simple formula whereby warming = TCRE x cumulative emissions implies a temperature response function to a CO_2 emission impulse that is approximated by a step function with amplitude equal to the TCRE. The temperature response function that best fits the CMIP5 ensemble in the experiment reported in Figure 1 has a mean amplitude of 1.72°C/TtC. This is for an equilibrium climate sensitivity of 3.1°C. FAIR has a mean amplitude of 1.77°C/TtC under 2015 conditions. Equilibrium climate sensitivity is the largest source of uncertainty about the TCRE. Matthews et al. (2009) found a 5-95% probability range of 1.0-2.1°C/TtC, Allen et al. (2009) found 1.4-2.5°C/TtC and Gillett et al. (2013) found 0.7-2.0°C/TtC based on the CMIP5 ensemble. Based on this and other evidence, IPCC adopted a 'likely' range of 1.0-2.1°C/TtC (Collins et al., 2013). Recently Nijsse et

well as being consistent with the climate science models for sound physical reasons, the linear warming-cumulative CO_2 relationship is also very simple and reduces the number of state variables needed to represent the climate system, which is advantageous for analytical models in particular.

All the models we have discussed are deterministic. But since the CMIP5 ensemble contains a lot of variation, and there are climate system uncertainties beyond what the CMIP5 ensemble captures, it may be useful to derive stochastic reduced-form models of the atmospheric carbon stock and temperature dynamics (e.g. van der Ploeg, 2018; Aengenheyster et al., 2018). One could then find, for example, the carbon budget compatible with a certain tolerance of overshooting the 2°C target (e.g. 1/3). Miftakhova et al. (2020) use a general emulation method for constructing low-dimensional stochastic approximations of complex climate models. Their best model gives a simple stochastic linear exponential lag model between temperature and cumulative CO_2 emissions. Alternatively, one could follow Pretis (2020), who builds on Kaufmann et al. (2011) and shows that energy-balance models of temperatures, ocean heat content and radiative forcing including greenhouse gases are equivalent to an econometric co-integrated system and can be estimated in discrete time. He shows that accounting for structural breaks from volcanic eruptions indicates large parameter uncertainties and that ignoring these breaks can lead to misleading policy implications due to model mis-specification. The model can then be used to quantify uncertainties in the dynamics of the atmospheric carbon stock and temperature.

IAMs tend to abstract from statistical and model uncertainty. We know that these uncertainties (especially the skewed distribution of the climate sensitivity and the effect of stochastic tipping points) can have large positive impacts on the optimal carbon price. To model such uncertainties properly, one cannot use the simple linear relationship between temperature and cumulative emissions, as this does not appear to hold at high temperatures (MacDougall, 2016), whilst in stochastic analysis one is interested in extreme outcomes even

al. (2020) have suggested 1.3-2.1°C/TtC based on the emerging results from CMIP6, with a most likely value of 1.68°C/TtC.

if they are quite unlikely. Future research should therefore be directed at finding reliable stochastic representations of the inherent statistical and modelling uncertainties in the CMIP5 ensemble and other ensembles. Only by accounting for the various forms of uncertainty will it be possible to find climate policies that are robust and prudent.

References

Aengenheyster, Matthias, Qing Yi Feng, Frederick Van Der Ploeg, and Henk A Dijkstra, "The point of no return for climate action," *Earth System Dynamics*, 2018, *9* (3).

Allen, Myles R, "Drivers of peak warming in a consumption-maximizing world," *Nature Climate Change*, 2016, *6*, 684–686.

_ , David J Frame, Chris Huntingford, Chris D Jones, Jason A Lowe, Malte Meinshausen, and Nicolai Meinshausen, "Warming caused by cumulative carbon emissions towards the trillionth tonne," *Nature*, 2009, *458* (7242), 1163–1166.

Arrow, Kenneth, Maureen Cropper, Christian Gollier, Ben Groom, Geoffrey Heal, Richard Newell, William Nordhaus, Robert Pindyck, William Pizer, Paul Portney et al., "Determining benefits and costs for future generations," *Science*, 2013, *341* (6144), 349–350.

Brock, William and Anastasios Xepapadeas, "Climate change policy under polar amplification," *European Economic Review*, 2017, *99*, 93–112.

Calel, Raphael and David A Stainforth, "On the physics of three integrated assessment models," *Bulletin of the American Meteorological Society*, 2017, *98* (6), 1199–1216.

Clarke, L., K. Jiang, K. Akimoto et al., "Asessing transformation pathways," in O. Edenhofer, R. Pichs-Madruga, Y. Sokona et al., eds., *Climate Change 2014: Mitigation of Climate Change. Contribution of Working Group III to the Fifth Assessment Report of the Intergovernmental Panel on Climate Change*, Cambridge, UK and New York, NY, USA: Cambridge University Press, 2014.

Collins, M., R. Knutti, J. Arblaster, J.-L. Dufresne, T. Fichefet, P. Friedlingstein, X. Gao, W.J. Gutowski, T. Johns, G. Krinner, M. Shongwe, C. Tebaldi, Weaver A.J., and M. Wehner,

"Long-term climate change: projections, commitments and irreversibility," in T.F. Stocker, C. Qin, G.-K. Plattner, M. Tignor, S.K. Allen, J. Boschung, A. Nauels, Y. Xia, V. Bex, and P.M. Midgeley, eds., *Climate Change 2013: The Physical Science Basis. Contribution of Working Group I to the Fifth Assessment Report of the Intergovernmental Panel on Climate Change*, Cambridge, UK and New York, NY, USA: Cambridge University Press, 2013.

Dietz, Simon and Frank Venmans, "Cumulative carbon emissions and economic policy: in search of general principles," *Journal of Environmental Economics and Management*, 2019, *96*, 108–129.

Friedlingstein, Pierre, Peter Cox, Richard Betts, Laurent Bopp, Werner von Bloh, Victor Brovkin, Patricia Cadule, Scott Doney, Michael Eby, Inez Fung et al., "Climate-carbon cycle feedback analysis: results from the C4MIP model intercomparison," *Journal of Climate*, 2006, *19* (14), 3337–3353.

Geoffroy, Olivier, David Saint-Martin, Dirk JL Olivié, Aurore Voldoire, Gilles Bellon, and Sophie Tytéca, "Transient climate response in a two-layer energy-balance model. Part I: Analytical solution and parameter calibration using CMIP5 AOGCM experiments," *Journal of Climate*, 2013, *26* (6), 1841–1857.

Gerlagh, Reyer and Matti Liski, "Consistent climate policies," *Journal of the European Economic Association*, 2018, *16* (1), 1–44.

Gillett, Nathan P, Vivek K Arora, Damon Matthews, and Myles R Allen, "Constraining the ratio of global warming to cumulative CO2 emissions using CMIP5 simulations," *Journal of Climate*, 2013, *26* (18), 6844–6858.

Gollier, Christian, *Pricing the Planet's Future: The Economics of Discounting in an Uncertain World*, Princeton University Press, 2012.

Golosov, Mikhail, John Hassler, Per Krusell, and Aleh Tsyvinski, "Optimal taxes on fossil fuel in general equilibrium," *Econometrica*, 2014, *82* (1), 41–88.

Hooss, Georg, Reinhard Voss, Klaus Hasselmann, Ernst Maier-Reimer, and Fortunat Joos, "A nonlinear impulse response model of the coupled carbon cycle-climate system (NICCS)," *Climate Dynamics*, 2001, *18* (3-4), 189–202.

Hope, Chris, "The marginal impact of CO2 from PAGE2002: An integrated assessment model incorporating the IPCC's five reasons for concern," *Integrated Assessment*, 2006, *6* (1).

_ , "The social cost of CO2 from the PAGE09 model," *Economics Discussion Papers*, 2011, (2011-39).

_ , "Critical issues for the calculation of the social cost of CO2: why the estimates from PAGE09 are higher than those from PAGE2002," *Climatic Change*, 2013, *117* (3), 531–543.

Interagency Working Group on Social Cost of Carbon, "Technical update on the social cost of carbon for regulatory impact analysis under executive order 12866," Technical Report, Interagency Working Group on Social Cost of Carbon, United States Government 2013.

IPCC, *Climate Change 2013: The Physical Science Basis. Contribution of Working Group I to the Fifth Assessment Report of the Intergovernmental Panel on Climate Change*, Cambridge, United Kingdom and New York, NY, USA: Cambridge University Press, 2013.

Joos, Fortunat, Raphael Roth, JS Fuglestvedt, GP Peters, IG Enting, W von Bloh, V Brovkin, EJ Burke, M Eby, NR Edwards et al., "Carbon dioxide and climate impulse response functions for the computation of greenhouse gas metrics: a multi-model analysis," *Atmospheric Chemistry and Physics*, 2013, *13* (5), 2793–2825.

Kaufmann, Robert K, Heikki Kauppi, Michael L Mann, and James H Stock, "Reconciling anthropogenic climate change with observed temperature 1998–2008," *Proceedings of the National Academy of Sciences*, 2011, *108* (29), 11790–11793.

Lemoine, Derek and Ivan Rudik, "Steering the climate system: using inertia to lower the cost of policy," *American Economic Review*, 2017, *107* (10), 2947–57.

Lenton, Timothy M, Hermann Held, Elmar Kriegler, Jim W Hall, Wolfgang Lucht, Stefan Rahmstorf, and Hans Joachim Schellnhuber, "Tipping elements in the Earth's climate system," *Proceedings of the National Academy of Sciences*, 2008, *105* (6), 1786–1793.

MacDougall, Andrew H, "The transient response to cumulative CO2 emissions: a review," *Current Climate Change Reports*, 2016, *2* (1), 39–47.

Maier-Reimer, Ernst and Klaus Hasselmann, "Transport and storage of CO_2 in the ocean: an inorganic ocean-circulation carbon cycle model," *Climate dynamics*, 1987, *2* (2), 63–90.

Manoussi, Vassiliki, Anastasios Xepapadeas, and Johannes Emmerling, "Climate engineering under deep uncertainty," *Journal of Economic Dynamics and Control*, 2018, *94*, 207–224.

Mattauch, Linus, H Damon Matthews, Richard Millar, Armon Rezai, Susan Solomon, and Frank Venmans, "Steering the climate system: Comment," *American Economic Review*, 2020, *110* (4), 1231–1237.

Matthews, H Damon, Nathan P Gillett, Peter A Stott, and Kirsten Zickfeld, "The proportionality of global warming to cumulative carbon emissions," *Nature*, 2009, *459* (7248), 829–832.

Miftakhova, Alena, Kenneth L Judd, Thomas S Lontzek, and Karl Schmedders, "Statistical approximation of high-dimensional climate models," *Journal of Econometrics*, 2020, *214* (1), 67–80.

Millar, Richard J, Zebedee R Nicholls, Pierre Friedlingstein, and Myles R Allen, "A modified impulse-response representation of the global near-surface air temperature and atmospheric concentration response to carbon dioxide emissions," *Atmospheric Chemistry and Physics*, 2017, *17* (11), 7213–7228.

Montamat, Giselle and James H Stock, "Quasi-experimental estimates of the transient climate response using observational data," *Climatic Change*, 2020, pp. 1–11.

Moss, Richard H, Jae A Edmonds, Kathy A Hibbard, Martin R Manning, Steven K Rose, Detlef P Van Vuuren, Timothy R Carter, Seita Emori, Mikiko Kainuma, Tom Kram et al., "The next generation of scenarios for climate change research and assessment," *Nature*, 2010, *463* (7282), 747–756.

National Academies of Sciences, Engineering, and Medicine, *Valuing Climate Damages: Updating Estimation of the Social Cost of Carbon Dioxide*, National Academies Press, 2017.

Nijsse, Femke JMM, Peter M Cox, and Mark S Williamson, "Emergent constraints on transient climate response (TCR) and equilibrium climate sensitivity (ECS) from historical warming in CMIP5 and CMIP6 models," *Earth System Dynamics*, 2020, *11* (3), 737–750.

Nordhaus, William D, "A review of the "Stern Review on the Economics of Climate Change"," *Journal of Economic Literature*, 2007, *45*, 686–702.

_ , "Estimates of the social cost of carbon: concepts and results from the DICE-2013R model and alternative approaches," *Journal of the Association of Environmental and Resource Economists*, 2014, *1* (1/2), 273–312.

_ , "Revisiting the social cost of carbon," *Proceedings of the National Academy of Sciences*, 2017, *114* (7), 1518–1523.

Pretis, Felix, "Econometric modelling of climate systems: The equivalence of energy balance models and cointegrated vector autoregressions," *Journal of Econometrics*, 2020, *214* (1), 256–273.

Quéré, Corinne Le, Robbie M. Andrew, Pierre Friedlingstein, Stephen Sitch, Judith Hauck, Julia Pongratz, Penelope A. Pickers, Jan Ivar Korsbakken, Glen P. Peters, Josep G. Canadell, Almut Arneth, Vivek K. Arora, Leticia Barbero, Ana Bastos, Laurent Bopp, Frédéric Chevallier, Louise P. Chini, Philippe Ciais, Scott C. Doney, Thanos Gkritzalis, Daniel S. Goll, Ian Harris, Vanessa Haverd, Forrest M. Hoffman, Mario Hoppema, Richard A. Houghton, George Hurtt, Tatiana Ilyina, Atul K. Jain, Truls Johannesen, Chris D. Jones, Etsushi Kato, Ralph F. Keeling, Kees Klein Goldewijk, Peter Landschützer, Nathalie Lefèvre, Sebastian Lienert, Zhu Liu, Danica Lombardozzi, Nicolas Metzl, David R. Munro, Julia E. M. S. Nabel, Shin ichiro Nakaoka, Craig Neill, Are Olsen, Tsueno Ono, Prabir Patra, Anna Peregon, Wouter Peters, Philippe Peylin, Benjamin Pfeil, Denis Pierrot, Benjamin Poulter, Gregor Rehder, Laure Resplandy, Eddy Robertson, Matthias Rocher, Christian Rödenbeck, Ute Schuster, Jörg Schwinger, Roland Séférian, Ingunn Skjelvan, Tobias Steinhoff, Adrienne Sutton, Pieter P. Tans, Hanqin Tian, Bronte Tilbrook, Francesco N. Tubiello, Ingrid T. van der Laan-Luijkx, Guido R. van der Werf, Nicolas Viovy, Anthony P. Walker, Andrew J. Wiltshire, Rebecca Wright, Sönke Zaehle, and Bo Zheng, "Global Carbon Budget 2018," *Earth System Science Data*, 2018.

Revelle, Roger and Hans E Suess, "Carbon dioxide exchange between atmosphere and ocean and the question of an increase of atmospheric CO2 during the past decades," *Tellus*, 1957, *9* (1), 18–27.

Ricke, Katharine L and Ken Caldeira, "Maximum warming occurs about one decade after a carbon dioxide emission," *Environmental Research Letters*, 2014, *9* (12), 124002.

Rose, Steven K, Delavane B Diaz, and Geoffrey J Blanford, "Understanding the social cost of carbon: a model diagnostic and inter-comparison study," *Climate Change Economics*, 2017, *8* (02), 1750009.

Solomon, Susan, Gian-Kasper Plattner, Reto Knutti, and Pierre Friedlingstein, "Irreversible climate change due to carbon dioxide emissions," *Proceedings of the National Academy of Sciences*, 2009, *106* (6), 1704–1709.

Stern, N., *The Economics of Climate Change: the Stern Review*, Cambridge University Press, 2007.

Stocker, T.F., D. Qin, G.-K. Plattner, L.V. Alexander, S.K. Allen, N.L. Bindoff, F.-M. Bréon, J.A. Church, U. Cubasch, S. Emori, P. Forster, P. Friedlingstein, N. Gillett, J.M. Gregory, D.L. Hartmann, E. Jansen, B. Kirtman, R. Knutti, K. Krishna Kumar, P. Lemke, J. Marotzke, V. Masson-Delmotte, G.A. Meehl, I.I. Mokhov, S. Piao, V. Ramaswamy, D. Randall, M. Rhein, M. Rojas, C. Sabine, D. Shindell, L.D. Talley, D.G. Vaughan, and S.-P. Xie, "Technical Summary," in T.F. Stocker, D. Qin, G.-K. Plattner, M. Tignor, S.K. Allen, J. Boschung, A. Nauels, Y. Xia, V. Bex, and P.M. Midgley, eds., *Climate Change 2013: The Physical Science Basis. Contribution of Working Group I to the Fifth Assessment Report of the Intergovernmental Panel on Climate Change*, Cambridge, United Kingdom and New York, NY, USA: Cambridge University Press, 2013.

van der Ploeg, Frederick, "The safe carbon budget," *Climatic Change*, 2018, *147* (1-2), 47–59.

_ **and Armon Rezai**, "The agnostic's response to climate deniers: Price carbon!," *European Economic Review*, 2019, *111*, 70–84.

van Vuuren, Detlef P, Jason Lowe, Elke Stehfest, Laila Gohar, Andries F Hof, Chris Hope, Rachel Warren, Malte Meinshausen, and

Gian-Kasper Plattner, "How well do integrated assessment models simulate climate change?," *Climatic Change*, 2011, *104* (2), 255–285.

Appendices for online publication

A Climate model experiments

A.1 Experimental protocol behind Figure 1

Figure 1 plots the temperature impulse response of climate science models and IAMs to an instantaneous emission of CO_2 of size 100GtC. We follow the experimental protocol of Joos et al. (2013). The background concentration of CO_2 in the atmosphere is initialised on the observed 2010 level, i.e. 389ppm or 829GtC.[22] We assume a pre-industrial atmospheric CO_2 concentration of 275.8ppm, resulting in an excess concentration of 113.2ppm in 2010.

For each of the 16 carbon cycle models that formed part of the CMIP5 study, the four-box carbon cycle model of Joos et al. (2013) is used as a reduced-form representation. Joos et al. (2013) document the fitting procedure and resulting parameter values. The initial excess atmospheric CO_2 concentration of 113.2ppm needs to be distributed among the four boxes of the Joos et al. model. The same need arises for the FAIR model, which shares the same four-box structure. Moreover, as the Joos et al. model was not designed to reproduce *historical* removal of CO_2 from the atmosphere (Millar et al., 2017), it is the FAIR model that we use to initialise the boxes in all of these models. To do this, we feed historical emissions into FAIR from 1890 to 2010.[23] This results in the following distribution of the initial excess concentration between the four boxes: 52.9% in box 1; 34.3% in box 2; 11.1% in box 3; 1.6% in box 4.

To keep the atmospheric CO_2 concentration constant after 2010, the experimental protocol of Joos et al. (2013) continues to add emissions. We compute these emissions as follows. The Joos et al. model implies that

$$\dot{m}_i = \psi_i E - \lambda_i m_i, \tag{8}$$

[22] We use a conversion rate of 100GtC = 46.9ppm throughout the paper.

[23] We obtain emissions between 1890 and 1990 from the EDGAR 1.4 database and between 1990 and 2010 from the SSP database.

where m_i is the carbon stock above pre-industrial in each box i, ψ_i is the proportion of emissions that enter each box and λ_i is the rate of removal of CO_2 from each box by carbon sinks. Constant atmospheric CO_2 therefore requires

$$\sum_i \dot{m}_i = 0 \Leftrightarrow E = \sum_i \lambda_i m_i. \tag{9}$$

Substituting (9) into (8) gives a solution for decay in each box:

$$\dot{m}_j = \psi_j \left[\sum_i \lambda_i m_i \right] - \lambda_j m_j. \tag{10}$$

As time goes by, carbon is transferred from the fast-decaying boxes in the model to the permanent box and in the steady state all carbon must be in the permanent box ($i = 1$). The same emissions path is used in simulations with all the carbon cycle models considered here.

The resulting background scenario is compared to a scenario with the same emissions path, but with an impulse of 100GtC added to the atmosphere at time zero (the year 2010). The 100GtC is added to each carbon box in proportion ψ_i.

The 16 CMIP5 carbon cycle models emulated by Joos et al. (2013) are then combined with 16 CMIP5 temperature models (i.e. atmosphere-ocean general circulation models), which are represented in reduced form using the model of Geoffroy et al. (2013), as described in their paper. We set the climate sensitivity equal to 3.1°C in all models.[24] This allows us to focus on temperature inertia in the climate models. For all models, we use 0.85°C as initial atmospheric warming relative to pre-industrial in 2010. The initial lower ocean temperature is 0.22°C above pre-industrial, obtained by running FAIR on historical emissions.

We now turn to the IAMs included in Figure 1. We take each of these models "off the shelf", except that, in order to be consistently compared following

[24]DICE assumes a climate sensitivity of 3.1°C. The mean climate sensitivity in Geoffroy et al. (2013) is between 3.05°C and 3.25°C, according to how models are aggregated ($\overline{\lambda} \times \overline{T_{CO_2 x2}} = 3.05°C$ while $\overline{\lambda \times T_{CO_2 x2}} = 3.25°C$). Default FAIR uses a climate sensitivity of 2.75°C.

the experimental protocol of Joos et al. (2013), we ensure all the models are initialised on the same atmospheric carbon stock and temperature:

- In DICE 2016, the carbon stocks are initialised on the year 2015, when the atmospheric CO_2 concentration is assumed to be 399.4ppm. Hence we reduce the excess carbon content of the three carbon boxes in DICE 2016 by 9.2% to obtain comparable 2010 initial conditions. We do not change the initial deep ocean temperature in DICE 2016.

- For the PAGE and FUND models, it is most convenient to slightly adjust the timing of the emission impulse so that the background CO_2 concentration is 389ppm – 2008 in FUND, 2009 in PAGE.

- For Golosov et al. (2014), we assume that 51.4% of the excess emissions in 2010 are in the permanent box and 48.6% are in the slow-decaying box. These numbers are obtained by using the authors' initial values in 2000 and running their model on historical emissions between 2000 and 2010.

- Gerlagh and Liski (2018) do not explicitly model temperature. CO_2 emissions map on to atmospheric concentrations and these in turn map directly on to damages. They define a common adjustment speed of temperature and damages in a one-box model. This gives $T_{t+1} = T_t - \varepsilon(ECS \times \log_2(M_t/M_{1850}) - T)$.

- For Lemoine and Rudik (2017), we can directly impute the initial atmospheric CO_2 concentration and temperature.

A.2 Variations on Figure 1

Figure 1 plotted the temperature response to an emission impulse of 100GtC, which is equivalent to about ten years of CO_2 emissions from burning fossil fuels at current rates (Le Quéré et al., 2018). Here we test the robustness of our findings to the size of the emission impulse by repeating the experiment with a much smaller impulse of 1GtC (Figure 6) and a much bigger

impulse of 1000GtC (Figure 7). We also test whether our findings hold when the background atmospheric CO_2 concentration is allowed to increase, rather than being held constant: in Figure 8, we plot the temperature response to an emission impulse of 100GtC on the IPCC RCP4.5 scenario. According to RCP4.5, the atmospheric CO_2 concentration in 2100 is around 550ppm. Arguably this best captures the world's current trajectory, absent further efforts to abate emissions in line with the UN temperature goals.

The temperature impulse response of the climate science models is fast (c. 10 years from emission to peak warming) in all cases. The corresponding temperature impulse response of the IAMs is always decades slower. It is important to point out that when the emission impulse is very large (e.g. 1000GtC as in Figure 7), or the background atmospheric CO_2 concentration is changing (e.g. along RCP4.5 as in Figure 8), carbon cycle feedbacks can become important in the long run. Hence we see in Figures 7 and 8 that the impulse response of FAIR deviates from that of Joos et al. (2013) (labelled the best fit of the CMIP5 ensemble as usual). FAIR is the benchmark in such experiments. It responds quickly to the emission impulse, but, instead of levelling of in the long run, temperature slowly increases due to weakening carbon sinks.

Figure 6: Dynamic temperature response of 256 climate science models (the CMIP5 ensemble), FAIR and seven IAMs to an instantaneous 1GtC emission impulse against a constant background atmospheric CO_2 concentration of 389ppm.

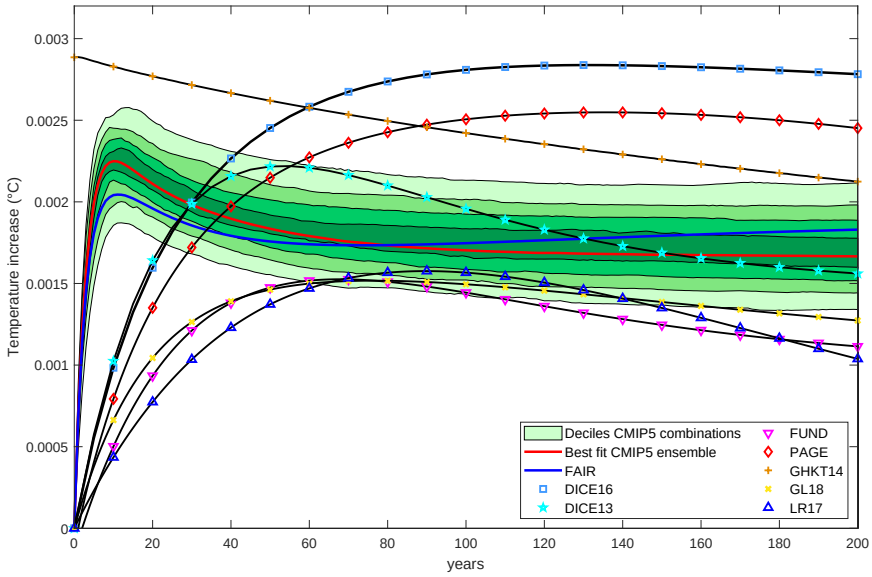

Figure 7: Dynamic temperature response of 256 climate science models (the CMIP5 ensemble), FAIR and seven IAMs to an instantaneous 1000GtC emission impulse against a constant background atmospheric CO_2 concentration of 389ppm.

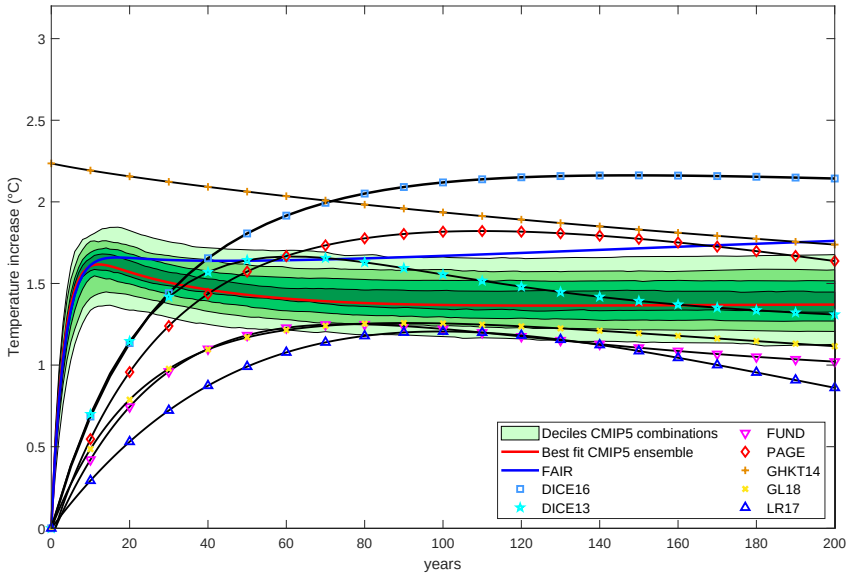

Figure 8: Dynamic temperature response of 256 climate science models (the CMIP5 ensemble), FAIR and seven IAMs to an instantaneous 100GtC emission impulse on an increasing atmospheric CO_2 concentration path. The emission is added when atmospheric CO_2 is 389ppm. Thereafter CO_2 emissions increase according to the IPCC RCP4.5 scenario.

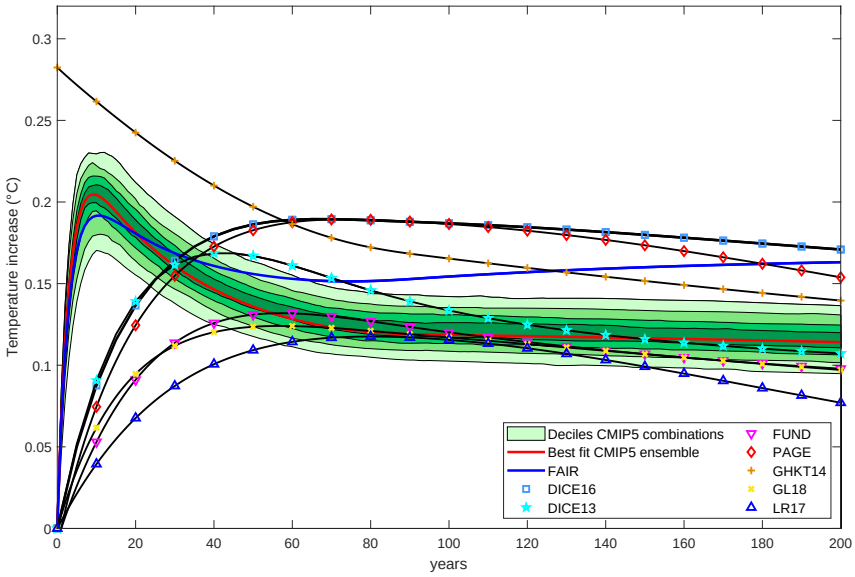

A.3 Experimental protocol behind Figure 2

Figure 2 relies on the FAIR model. FAIR is identical to the model of Joos et al. (2013), except the residence time of CO_2 in each of the four atmospheric boxes is modified by a parameter α representing carbon cycle feedbacks. FAIR calculates α as a function of the integrated CO_2 impulse response function (iIRF) over the first 100 years of the model horizon. Over this period, the iIRF has a linear relationship with both temperature and cumulative CO_2

emissions absorbed by carbon sinks:

$$\text{iIRF}_{100} = r_{pi} + r_T T + r_C \left[\sum_{s=pi}^{t} E_s - (M_s - M_{pi}) \right] \tag{11}$$

where $r_{pi} = 34.4$ years is the estimated pre-industrial value of iIRF_{100}, $\sum_{s=pi}^{t} E_s$ denotes cumulative CO_2 emissions since pre-industrial, $r_T = 4.165$ years/°C and $r_C = 0.019$ years/GtC. The assumed relationship between α and iIRF_{100} in FAIR has no analytical solution, but can be well approximated by fitting an exponential function, which results in the following solution:

$$\alpha = 0.0107 \exp\left(0.0866 \text{iIRF}_{100}\right). \tag{12}$$

Figure 2 shows yearly carbon uptake by sinks as a function of the atmospheric CO_2 concentration for constant emissions of 39.1GtCO_2 and constant non-CO_2 forcing of 0.181W/m^2, which correspond to 2015 forcing in the SSP database.[25] To make the graph, we use 2015 initial conditions, with 263GtC in the atmosphere (as in DICE) and 0.85°C warming (also as in DICE). For FAIR, we use the same relative distribution among the four boxes as above and 0.28°C deep ocean warming.

A.4 Experimental protocol behind Figures 3 and 4

Figure 3 is generated using exactly the same procedure as Figure 1, but reports the difference in atmospheric CO_2 concentration instead of the difference in temperature.

Figure 4 uses the same background scenario as Figure 1. This is compared to a scenario with a constant CO_2 concentration of 436ppm (398ppm+100GtC) from 2010 onwards.

[25] Hosted by the IIASA Energy Program at https://tntcat.iiasa.ac.at/SspDb.

B Further details on carbon cycle and warming models

B.1 Linear models of the carbon cycle

The linear carbon cycle is described by n difference equations, where $\mathbf{m}_t$ is a vector whose elements contain the amount of carbon in each box at time t, $\mathbf{A}$ is a square matrix of constants and $\mathbf{b}$ is a column vector. Let $\mathbf{d}$ be the vector that maps the contents of the various boxes into the stock of atmospheric carbon, i.e.

$$M_t \equiv \mathbf{d}'\mathbf{m}_t = \mathbf{d}' \left[\mathbf{A}^t M_0 + \sum_{s=1}^{t} \mathbf{A}^{t-s} \mathbf{b} E_s \right].$$

Spectral decomposition yields $\mathbf{A} = \mathbf{V}\mathbf{\Lambda}\mathbf{V}^{-1}$, where the diagonal matrix contains the eigenvalues in decreasing order of magnitude along its diagonal and the columns of the n x n matrix $\mathbf{V}$ contain the linearly independent eigenvectors (assuming all eigenvalues are real and distinct). Given that the columns of $\mathbf{A}$ must sum to one, the first of the n eigenvalues equals 1 and the others are between zero and one (provided the system is stable). We have

$$M_t = \mathbf{d}'\mathbf{V} \left[\mathbf{\Lambda}^t \mathbf{V}^{-1} M_0 + \sum_{s=1}^{t} \mathbf{\Lambda}^{t-s} \mathbf{V}^{-1} \mathbf{b} E_s \right].$$

The effect of a change in the emissions path from some reference path on the corresponding change in the stock of atmospheric carbon is independent of M_0 and given by

$$\Delta M_t = \mathbf{d}'\mathbf{V} \sum_{s=1}^{t} \mathbf{\Lambda}^{t-s} \mathbf{V}^{-1} \mathbf{b} \Delta E_s.$$

Define $\bar{\mathbf{d}} \equiv \mathbf{V}'\mathbf{d}$ and $\bar{\mathbf{b}} \equiv \mathbf{V}^{-1}\mathbf{b}$, so that

$$\Delta M_t = \sum_{s=1}^{t} \sum_{i=1}^{n} \psi_i {\lambda_i}^{t-s} \Delta E_s,$$

where $\psi_i \equiv \bar{b}_i \bar{d}_i$ is the contribution of each box to the atmospheric carbon stock and the λ_i are the eigenvalues of the matrix $\mathbf{A}$. The impulse response

function shows the effects of a small impulse in the first period only and equals

$$\frac{\Delta M_t}{\Delta E_1} = \sum_{i=1}^{n} \psi_i {\lambda_i}^{t-1}.$$

The first eigenvalue is 1 whenever a proportion of emissions ψ_i stays in the atmosphere forever. In such cases, the impulse response is the sum of its permanent and transitory components, i.e.

$$\frac{\Delta M_t}{\Delta E_1} = \psi_1 + \sum_{i=2}^{n} \psi_i {\lambda_i}^{t-1}.$$

The FUND model

The FUND carbon cycle model, which is based on Maier-Reimer and Hasselmann (1987), has 5 boxes with shares of emissions flowing into each of them equal to $\mathbf{b} = (0.13, 0.20, 0.32, 0.25, 0.1)'$, $\mathbf{d} = (1, 1, 1, 1, 1)'$ and $\mathbf{A}$ has diagonal elements equal to exp(-1/lifetime), where the lifetimes for the 5 boxes are ∞, 363, 74, 17 and 2 years respectively. These correspond to half-lives of ∞, 252, 51, 12 and 1.4 years respectively.

The Golosov et al. (2014) carbon cycle model: 2 boxes

Golosov et al. (2014) have $\mathbf{A} = \begin{pmatrix} 1 & 0 \\ 0 & 1-\varphi \end{pmatrix}$, $\mathbf{b} = \begin{pmatrix} \theta_L \\ \theta_0(1-\theta_L) \end{pmatrix}$ and $\mathbf{d} = \begin{pmatrix} 1 \\ 1 \end{pmatrix}$, where $0 < \theta_L < 1$ and $1 - \theta_L$ are the proportions of emissions that flow into the boxes holding the permanent and transitory components of atmospheric carbon respectively, $0 < \theta_0 < 1$ is the proportion of atmospheric carbon in the transitory box that decays within the span of a unit of time (i.e. within a decade), and $\varphi > 0$ denotes the speed of decay of carbon in the transitory box. Hence Eq. (3) becomes

$$M_t = m_0(1) + (1-\varphi)^t m_0(2) + \sum_{s=1}^{t} \left[\theta_L + \theta_0(1-\theta_L)(1-\varphi)^{t-s}\right] E_s,$$

where the term in square brackets shows how much of an emission impulse at time s is left in the atmosphere at time t. Roughly a fifth of carbon stays up in the atmosphere "forever", half of an emission impulse is removed after 30 years, and the remaining carbon in the atmosphere has a mean life of 300 years. This yields $\theta_L = 0.2$, $\theta_0 = 0.393$ and $\varphi = 0.0228$. It follows that the half-life equals $\ln(0.5)/\ln(0.9772) = 30$ decades. The initial values for 2010 are $S_0(1) = 684$GtC and $S_0(2) = 118$GtC. Our starting date is 2015, so we update these and use $S_0(1) = 712$GtC and $S_0(2) = 159$GtC instead.

The DICE 2016 carbon cycle model: 3 boxes

The DICE 2016 carbon cycle of Nordhaus (2017) has three boxes: (1) the atmosphere, (2) the upper oceans and biosphere, and (3) the lower/deep oceans. The diffusion matrix is

$$\mathbf{A} = \begin{pmatrix} 0.88 & 0.196 & 0 \\ 0.12 & 0.797 & 0.001465 \\ 0 & 0.007 & 0.998535 \end{pmatrix}$$

and $\mathbf{b} = \mathbf{d} = (1, 0, 0)'$. No carbon leaves the system, so the elements of the columns of $\mathbf{A}$ sum to 1. The rate of uptake by the biosphere and oceans is independent of the amount of carbon stored in each box, so positive feedback between atmospheric CO_2 and CO_2 uptake is ruled out. There is no direct interchange of carbon between the atmosphere and the lower/deep oceans. The lower/deep oceans can store a large amount of carbon, but the rate of diffusion into the lower/deep oceans is only 0.007. The eigenvalues of $\mathbf{A}$ are (0.6796, 0.9959, 1) and

$$\mathbf{V} = \begin{pmatrix} 0.6991 & 0.5075 & 0.3173 \\ -0.7148 & 0.3002 & 0.1942 \\ 0.0157 & -0.8077 & 0.9282 \end{pmatrix},$$

so $\bar{\mathbf{b}} = (0.5283, 0.8085, 0.6946)'$, $\bar{\mathbf{d}} = (0.6991, 0.5075, 0.3173)'$ and thus the ψ_i are 37%, 41% and 22%. Since no carbon leaves the boxes, one of the

eigenvalues equals 1. The smallest eigenvalue corresponds to a half-life of 9 years (5 x $\ln(0.5)/\ln(0.6796)$) and the middle one corresponds to a half-life of 851 years.

The DICE 2013 carbon cycle model

The DICE 2013 carbon cycle has the same structure as DICE 2016. The diffusion matrix is

$$\mathbf{A} = \begin{pmatrix} 0.912 & 0.0383 & 0 \\ 0.088 & 0.9592 & 0.0003 \\ 0 & 0.0025 & 0.9997 \end{pmatrix}.$$

The eigenvalues of $\mathbf{A}$ are (0.8729, 0.99793, 1) and the ψ_i are 69%, 26% and 5%. The smallest eigenvalue corresponds to a half-life of 26 years and the middle one corresponds to a half-life of 1675 years.

The Gerlagh and Liski (2018) carbon cycle model: 3 boxes

Gerlagh and Liski (2018) have boxes for (i) the atmosphere and the upper oceans, (ii) the biosphere and (iii) the lower oceans. Since within a decade (their unit of time) carbon mixes perfectly between the atmosphere and the upper oceans, these are combined into box one. The stock of atmospheric carbon is a constant share of the contents of box one, i.e. $\mathbf{d} = (0.914, 0, 0)'$. They have

$$\mathbf{A} = \begin{pmatrix} 0.6975 & 0.2131 & 0.029 \\ 0.1961 & 0.7869 & 0 \\ 0.1063 & 0 & 0.9706 \end{pmatrix}$$

and $\mathbf{b} = (0.8809, 0.0744, 0.0447)'$. The eigenvalues of $\mathbf{A}$ are 0.5286, 0.9264 and 1, and we calculate the corresponding ψ_i to be 44.5%, 18.2% and 16.2%. The eigenvalues imply that the half-lives for the two temporary boxes are 90 and 11 years respectively.

The Joos et al. (2013) carbon cycle model: 4 boxes

Joos et al. (2013) use a continuous-time model with one permanent and three transitory boxes to fit impulse response functions to an ensemble of Earth System model simulations.[26] Their best fit of the CMIP5 ensemble is

$$\mathbf{A} = \begin{pmatrix} 1 & 0 & 0 & 0 \\ 0 & 0.9975 & 0 & 0 \\ 0 & 0 & 0.9730 & 0 \\ 0 & 0 & 0 & 0.7927 \end{pmatrix},$$

$\mathbf{b} = (0.2173, 0.2240, 0.2824, 0.2763)'$ and $\mathbf{d} = (1, 1, 1, 1)'$ on an annual basis. The mean lags for the temporary boxes are 277, 25 and 3 years. Aengenheyster et al. (2018) also estimate a 4-box model in continuous time.

The Delay 56 and Delay 112 carbon cycle models use the same values as Joos et al. (2013) for ψ, but multiply the mean lags by five and ten respectively. In other words, any point on the impulse response function will be a point on the Delay 56 (112) impact response function five (ten) years later.

The PAGE model

The PAGE09 carbon cycle model (Hope, 2006, 2011, 2013) can be approximated using three boxes with shares of emissions flowing into each of them equal to $\mathbf{b} = (0.19, 0.43, 0.38)'$ and $\mathbf{d} = (1, 1, 0)'$, and $\mathbf{A}$ has diagonal elements equal to exp(-1/lifetime), where the lifetimes for the 3 boxes are ∞, 73.33 and close to 0 years respectively. A feedback from temperature to carbon concentration is introduced in PAGE09, which scales up the concentration from the dynamic system by a 'gain' factor to compute forcing in that year. The gain factor does not, however, influence the evolution of carbon stocks. This feedback, which models the decreasing absorptive capacity of oceans and potentially that of soil, is a linear relation of temperature (with an uncertain constant of median 9.67%/°C). However, a maximum of 53.33% can be added to the atmospheric carbon concentration.

[26] In continuous time, their model is $\dot{\mathbf{m}} = \mathbf{b}E - (\mathbf{A} - \mathbf{I})\,\mathbf{m}$.

B.2 Temperature dynamics models

In parallel to the analysis of the carbon cycle above, let temperature be given by $T_t = \mathbf{d}'\mathbf{m}_t$, where the vector $\mathbf{m}_t$ follows from the linear system $\mathbf{m}_t = \mathbf{A}\mathbf{m}_{t-1} + \mathbf{b}F_t$. Using spectral decomposition, $\mathbf{A} = \mathbf{V}\mathbf{\Lambda}\mathbf{V}^{-1}$ and defining $\bar{\mathbf{d}} \equiv \mathbf{V}'\mathbf{d}$ and $\bar{\mathbf{b}} \equiv \mathbf{V}'\mathbf{b}$, we can solve for

$$T_t = \bar{\mathbf{d}}\left(\mathbf{\Lambda}^t\mathbf{V}^{-1}T_0 + \sum_{s=1}^{t}\mathbf{\Lambda}^{t-s}\bar{\mathbf{b}}F_s\right) = \bar{\mathbf{d}}'\mathbf{\Lambda}^t\mathbf{V}^{-1}T_0 + \sum_{s=1}^{t}\sum_{i=1}^{2}\psi_i^T\lambda_i^{T\,t-s}F_s,$$

where $\psi_i^T \equiv \bar{b}_i\bar{d}_i$, $i = 1, 2$. It follows that the temperature response to a step increase in forcing, $F_s = \Delta F, \forall s \geq 1$, and to an increase in initial temperature, equals

$$\Delta T_t = \bar{\mathbf{d}}'\mathbf{\Lambda}^t\mathbf{V}^{-1}T_0 + \left[\sum_{i=1}^{2}\frac{\psi_i^T}{(1-\lambda_i^T)}\left(1-\lambda_i^{T\,t}\right)\right]\Delta F.$$

Note that the effects of initial temperature and a change in forcing can be added for linear systems (the superposition principle).

Geoffroy et al. (2013)

Geoffroy et al. (2013) have a two-box model for temperature dynamics in continuous time,

$$\dot{T} = \frac{1}{C}\left[F - \lambda T - \gamma(T - T_{LO})\right]$$

and

$$\dot{T}_{LO} = \frac{\gamma}{C_0}(T - T_{LO}),$$

where $C = 7.3$ W yr m^{-2} K^{-1} is the effective heat capacity of the upper/mixed ocean layer, $C_0 = 106$ W yr m^{-2} K^{-1} is the effective heat capacity of the deep oceans, $\lambda = 1.13$ W m^{-2} K^{-1} and $\gamma = 0.73$ W m^{-2} K^{-1}. These are the values that best fit the multi-model mean of the CMIP5 ensemble. There is a box T representing the mean temperature of the atmosphere, land and upper oceans, and a box T_{LO} representing the mean temperature of the deep oceans. Steady-state temperature corresponding to constant forcing F is $T = T_{LO} = F/\lambda$, which gives an equilibrium climate sensitivity or ECS (i.e. the steady-state increase in

temperature resulting from doubling the atmospheric stock of CO_2 relative to pre-industrial) of $F_{2\times CO_2}/\lambda$= 3.45/1.13 = 3.05 K given $F_{2\times CO_2} = 3.45$ W m^{-2}. To get an ECS of 3.1, we adjust by multiplying $F_{2\times CO_2}$ by the factor 3.1/3.05 and modify the first equation to $\dot{T} = \frac{1}{C}\left[(3.1/3.05)F - \lambda T - \gamma(T - T_{LO})\right]$.

The state transition matrix $\mathbf{A} = \begin{pmatrix} -(\lambda+\gamma)/C & \gamma/C \\ \gamma/C_0 & -\gamma/C_0 \end{pmatrix}$, which has eigenvalues -0.2575 and -0.0041. Using $\mathbf{d} = (1,0)'$ and $\mathbf{b} = (1/C, 0)'$, we obtain $\psi_1^T = 0.135$ and $\psi_2^T = 0.0015$, which gives the following impulse response function:

$$\frac{\Delta T(t)}{\Delta F(s)} = 0.135\exp(-0.2575(t-s)) + 0.0015\exp(-0.0041(t-s)).$$

Notice ψ_1^T is much larger than ψ_2^T, i.e. the system responds quickly to an impulse of forcing. Since the lower ocean has a large heat capacity, it quickly absorbs the extra heat in the atmosphere.

By contrast, the reaction to a step increase in forcing ΔF is slower. The temperature increase for a step increase in forcing beginning at time s, with a steady-state temperature effect of $\Delta F/\lambda$, is

$$\frac{\Delta T(t)}{\Delta F} = \frac{1}{\lambda}\left[1 - 0.523\exp(-0.2575(t-s)) - 0.366\exp(-0.0041(t-s))\right].$$

This formula is based on the same eigenvalues, but the relative weight on the slow box is much larger: $\hat{\psi}_1^T = 0.523$ versus $\hat{\psi}_2^T = 0.366$. With constant forcing, the deep ocean reaches the same steady-state temperature as the atmosphere, but, given the large heat capacity of the deep ocean, it takes much longer to reach.

For the Delay 56 and Delay 112 model versions, we multiply the capacities C and C_0 by factors of 5 and 10 respectively. This does not affect the values of ψ_i^T. However, the Delay 56 system has eigenvalues of -0.0515 and -0.0008; the Delay 112 system -0.0258 and -0.0004. In other words, half-lives are multiplied by 5 and 10 for the Delay 56 and Delay 112 variants respectively.

DICE 2016

DICE 2016 is formulated in discrete time with a time unit of 5 years and, like the model of Geoffroy et al. (2013), has two heat boxes, one for the temperature of the atmosphere, land and upper oceans, and one for the temperature of the deep oceans:

$$T_t = T_{t-1} + \frac{1}{C_{UP}}\left[F_t - \frac{3.6813}{ECS}T_{t-1} - 0.088(T_{t-1} - T_{LO,t-1})\right]$$

and

$$T_{LO,t} = T_{LO,t-1} + \frac{0.088}{C_{LO}}(T_{t-1} - T_{LO,t-1}),$$

where $C_{UP} = 1/0.1005$ W yr m^{-2} K^{-1} and $C_{LO} = 0.088/0.025$ W yr m^{-2} K^{-1} are the effective heat capacities of the upper and lower oceans respectively, and 0.088 and 0.025 are the coefficients of heat exchange between the upper and deep oceans respectively. The steady state temperature is $T_t = T_{LO,t} = ECS \times F_t/3.6813 = 0.842F_t$, where ECS is set to 3.1 K. The transient climate sensitivity is set to 1.7 K. The transition matrix $\mathbf{A} = \begin{pmatrix} 0.873 & 0.009 \\ 0.025 & 0.975 \end{pmatrix}$, $\mathbf{b} = (1/C_{UP}, 0)'$ and $\mathbf{d} = (1, 0)'$. This yields eigenvalues 0.871 and 0.977 with corresponding shares $\psi_1^T = 0.0985$ and $\psi_2^T = 0.002$. Note that $\psi_1^T + \psi_2^T = 1/C_{UP} = 0.1005$. The temperature response to an impulse in forcing is $\frac{\Delta T_t}{\Delta F_1} = 0.0985 \times 0.8711^{t-1} + 0.0022 \times 0.9771^{t-1}$. The temperature response to a step increase in forcing at time s equals

$$\frac{\Delta T_t}{\Delta F} = \sum_{i=1}^{2}\left(\frac{\psi_i^T \lambda_i^{T\,t}}{1 - \lambda_i^{T\,t}}\right) = \frac{0.0985 \times (1 - 0.871^t)}{0.129} + \frac{0.002 \times (1 - 0.977^t)}{0.003}.$$

We find that $\lim_{t\to\infty} \frac{\Delta T_t}{\Delta F} = \sum_{i=1}^{2} \frac{\psi_i^T}{\lambda_i^T} \to \frac{0.0985}{0.129} + \frac{0.002}{0.003} = 0.8521$.

DICE 2013

DICE 2013's warming model is almost identical to DICE 2016. The transition matrix is $\mathbf{A} = \begin{pmatrix} 0.863 & 0.009 \\ 0.025 & 0.975 \end{pmatrix}$. This yields eigenvalues 0.861 and 0.977 with

corresponding shares $\psi_1^T = 0.0989$ and $\psi_2^T = 0.002$.

Golosov et al. (2014)

Golosov et al. (2014) have no temperature lag, so they have $T_t = 0.842F_t$.

Gerlagh and Liski (2018)

Gerlagh and Liski (2018) have a simple lag with partial adjustment of 0.183 per decade (or 2% per year), so they have

$$T_t = T_{t-1} + 0.183\ (0.842F_t - T_{t-1}).$$

This corresponds to a half-life of 34 years. Although this long lag is in line with the scientific evidence of some time ago (Solomon et al., 2009), it does not accord with more recent scientific evidence (e.g Geoffroy et al., 2013). The resulting temperature response to an impulse in forcing is $\frac{\Delta T_t}{\Delta F_1} = 0.842 \times 0.817^{t-1}$. The corresponding response to a step increase in forcing is

$$\frac{\Delta T_t}{\Delta F} = 0.842 \times \frac{1 - 0.817^t}{0.183}.$$

FUND

The annual FUND model also has a simple temperature lag, but with a partial adjustment coefficient of 0.0224 per year, corresponding to a mean lag of 44.6 years and a half-life of 30.6 years.

PAGE

Global mean temperature in PAGE09 is the weighted sum of regional temperatures. Once aggregated, however, global temperature follows a median life-time of 24 years (and mean of 50 years).

B.3 Convoluted temperature impulse response function

Equation (9) gives the convoluted temperature impulse response function, which is derived from the carbon stock impulse response function, the temperature-forcing response function, and

$$\frac{\partial T_s}{\partial M_s} = \frac{F_{2\times CO_2}}{\ln 2}\frac{1}{M_s}.$$

The temperature response to a small step change in the stock of atmospheric carbon, $\Delta M_s = \Delta M,\ \forall M \geq 0$, is thus

$$\frac{\Delta T_t}{\Delta M} = \frac{F_{2\times CO_2}}{\ln 2}\frac{1}{M_0}\frac{\Delta T_t}{\Delta F}$$

for the Geoffroy et al. (2013) model and

$$\frac{\Delta T_t}{\Delta M} = \frac{F_{2\times CO_2}}{\ln 2}\frac{1}{M_1}\frac{\Delta T_t}{\Delta F}$$

for the discrete-time models such as DICE. Note that the response to a step increase in atmospheric carbon decreases in the values of the atmospheric carbon stock. To calculate these convoluted step responses, we suppose that the concentration of atmospheric carbon stays constant at its initial value. Hence we set M_s to 3038 GtCO2 or 389 ppmv for all s. For the DICE model we thus get $\frac{\Delta T_t}{\Delta M} = \frac{F_{2\times CO_2}}{\ln 2}\frac{1}{M_1}\frac{\Delta T_t}{\Delta F} = 0.0012585$ as $t \to \infty$. For a small step change in atmospheric carbon of 100GtC, the steady-state increase in temperature would then equal $0.0012585 \times 100 \times 44/12 = 0.46$ K, which is consistent with the plot in Figure 4.

C Further results

DICE 2016 compared with DICE-FAIR-Geoffroy

Here we compare standard DICE 2016 (row 5) with DICE-FAIR-Geoffroy (row 1). This comparison is affected by differences in: (a) temperature dynamics

between the DICE 2016 and Geoffroy et al. (2013) models; (b) removal of atmospheric CO_2 between the DICE 2016 and Joos et al. (2013) carbon cycles, and; (c) assumptions about (non-)diminishing marginal removal of atmospheric CO_2 between DICE 2016/Joos et al. (2013) and FAIR. Therefore this comparison is of the combined effect of all the modifications to DICE that we have identified, which would bring it fully into line with the climate science models we have assembled.

The combined effect of these is a higher optimal carbon price in DICE 2016 than in DICE-FAIR-Geoffroy (see Figure 5). The 2020 optimal carbon price is 24% higher in DICE 2016. Yet it is on the 2°C cost-minimising paths that we see the largest price differences. The 2020 2°C cost-minimising carbon price is three times higher in DICE 2016 than in DICE-FAIR-Geoffroy, resulting in a reduction in 2020 emissions of almost $9GtCO_2$. Yet, despite lower emissions throughout this century on both the optimal and 2°C cost-minimising paths, temperatures end up being higher in DICE 2016, by more than 0.5°C in 2100 on the optimal path. The main driver of these differences is the tendency of DICE 2016 to heat up too much in the long run, as the analysis just below will show. This is particularly manifest on the 2°C cost-minimising path, because heating up too much in the long run makes it extremely difficult to avoid the global mean temperature exceeding 2°C above the pre-industrial level.

A method of apportioning the differences between DICE 2016 and DICE-FAIR-Geoffroy to factors (a) to (c) is to plot the percentage difference in carbon prices and temperatures – always relative to DICE-FAIR-Geoffroy – in DICE 2016, DICE-Geoffroy (i.e. combining the DICE 2016 carbon cycle with the Geoffroy et al. (2013) temperature dynamics model), DICE-Joos (i.e. combining the Joos et al. (2013) carbon cycle with the DICE 2016 temperature dynamics model) and DICE-Joos-Geoffroy. Figure 9 does this.[27] The way to intuit this figure is that whichever model is closest to DICE 2016 explains most of the difference between it and DICE-FAIR-Geoffroy. Hence the main contributing factor to the difference in *optimal* carbon prices between DICE

[27]For this comparison we omit emissions, because when emissions approach or reach zero the differences between the models can explode or be undefined respectively.

2016 and DICE-FAIR-Geoffroy is (b) insufficient removal of atmospheric CO_2 in DICE 2016 (top left panel). This is a feature shared by DICE 2016 and DICE-Geoffroy, but not by the other models, which incorporate the four-box carbon cycle of Joos et al. (2013). However, when it comes to the 2°C carbon price, or temperature on either path, the main contributing factor to the difference between DICE 2016 and DICE-FAIR-Geoffroy is (a) temperature dynamics. Excessive delay, offset by excessive long-term warming, is a feature shared by the DICE 2016 and DICE-Joos variants. Excessive delay and excessive long-term warming are responsible for the temperature trajectories in DICE 2016 that start below DICE-FAIR-Geoffroy but end up higher, significantly so on the optimal path. Excessive long-term warming also explains the high 2°C carbon price, because it significantly limits the 2°C carbon budget.

Figure 9: Price and temperature paths relative to the benchmark DICE-FAIR-Geoffroy model. Left column – welfare-maximising path; right column – cost-effective path to limit warming to 2°C. Top row – carbon prices; bottom row – warming. Whichever model is closest to DICE 2016 explains most of the difference between it and DICE-FAIR-Geoffroy.

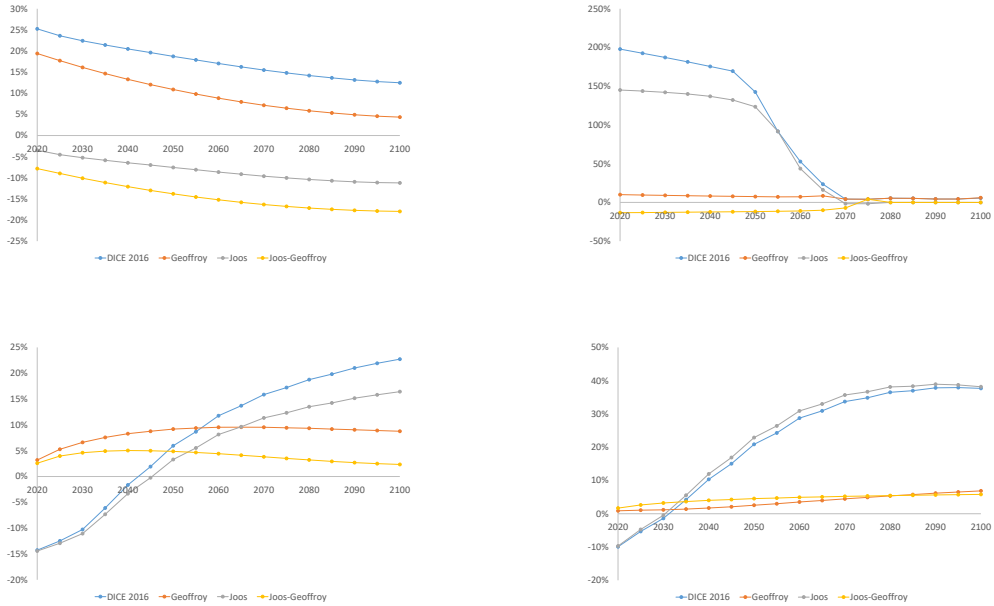

2°C cost minimisation under different exogenous emissions/forcing scenarios

Figure 10 shows using DICE-FAIR-Geoffroy that limiting warming to 2°C is much more costly when exogenous CO_2 emissions/forcing come from standard DICE 2016 than when they come from the IPCC's RCP2.6 scenario. The former scenario was designed to apply no matter the amount of CO_2 emissions abatement undertaken in the model (i.e. from the energy sector), while the latter was designed by IPCC to imply a level of abatement outside CO_2/energy that is consistent with the 2°C goal. Limiting warming to 2°C is infeasible in DICE 2016 with standard DICE 2016 exogenous emissions/forcing.

Figure 10: 2°C cost-minimising carbon prices in DICE-FAIR-Geoffroy using two alternative scenarios for emissions of CO_2 from land use and forestry, and exogenous radiative forcing from other greenhouse gases and agents. Carbon prices are much higher under the standard DICE 2016 scenario than under the RCP2.6 scenario.

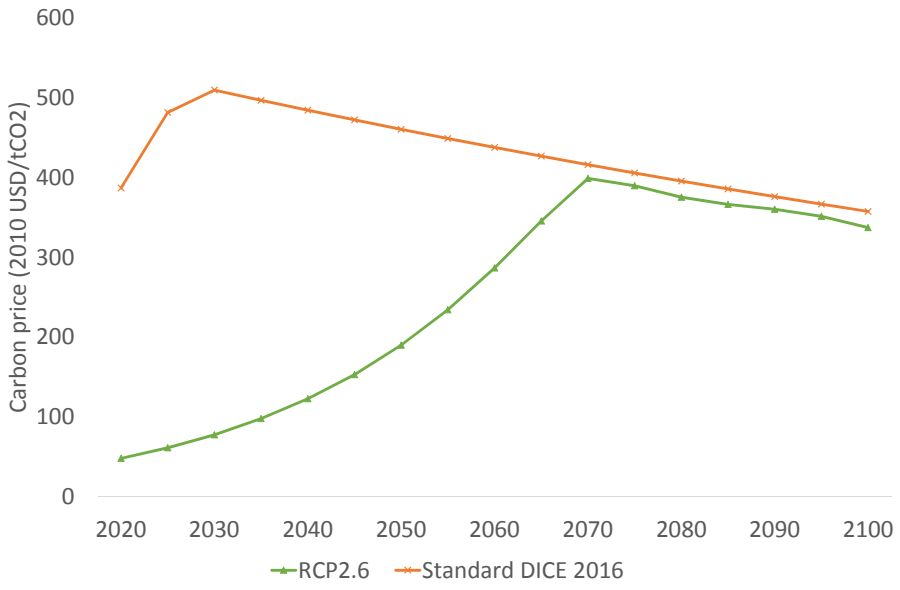

D GAMS code for DICE 2016 with the FAIR carbon cycle and the Geoffroy et al. (2013) temperature model

In this section we provide GAMS code to implement the FAIR carbon cycle in DICE 2016, as well as parameters to implement the Geoffroy et al. (2013) warming model. This replaces the three-box model of the carbon cycle and the two-box temperature model of standard DICE 2016.

```
$ontext
This is a modified version of DICE-2016R-091916ap.gms.
The carbon cycle has been changed to the four box model of Joos et al. and parameters of thermal
dynamics to match Geoffroy et al. The positive feedback from sink satiation has been added. See
**-comments for details throughout.

$title        DICE-2016R September 2016 (DICE-2016R-091216a.gms)
$offtext

set        t  Time periods (5 years per period)                    /1*100/

PARAMETERS
** Availability of fossil fuels
        fosslim  Maximum cumulative extraction fossil fuels (GtC)  /6000/
**Time Step
        tstep    Years per Period                                  /5/
** If optimal control
        ifopt    Indicator where optimized is 1 and base is 0      /0/
        ifmiulim Indicator where fixed miu('1') is 1 and 0 else    /1/
** Preferences
        elasmu   Elasticity of marginal utility of consumption     /1.45 /
        prstp    Initial rate of social time preference per year   /.015  /
**new parameters for public decision making
        elasmu_pub   Elasticity of marginal utility of consumption     /1.45 /
        prstp_pub    Initial rate of social time preference per year   /.015  /

** Population and technology
        gama     Capital elasticity in production function        /.300    /
        pop0     Initial world population 2015 (millions)         /7403    /
        popadj   Growth rate to calibrate to 2050 pop projection  /0.134   /
        popasym  Asymptotic population (millions)                 /11500   /
        dk       Depreciation rate on capital (per year)          /.100    /
        q0       Initial world gross output 2015 (trill 2010 USD) /105.5   /
        k0       Initial capital value 2015 (trill 2010 USD)      /223     /
        a0       Initial level of total factor productivity       /5.115    /
        ga0      Initial growth rate for TFP per 5 years          /0.076   /
        dela     Decline rate of TFP per 5 years                  /0.005   /
** Emissions parameters
        gsigma1  Initial growth of sigma (per year)                  /-0.0152 /
        dsig     Decline rate of decarbonization (per period)        /-0.001  /
        eland0   Carbon emissions from land 2015 (GtCO2 per year)    / 2.6    /
        deland   Decline rate of land emissions (per period)         / .115   /
        e0       Industrial emissions 2015 (GtCO2 per year)          /35.85    /
        miu0     Initial emissions control rate for base case 2015   /.03     /
** Carbon cycle
** new carbon cycle replaces DICE's oceanic carbon reservoirs with four atmospheric carbon
boxes. Transition matrix is diagonal since it is a reduced-form model.
$ontext
* Initial Conditions
        mat0   Initial Concentration in atmosphere 2015 (GtC)       /851    /
        mu0    Initial Concentration in upper strata 2015 (GtC)     /460    /
        ml0    Initial Concentration in lower strata 2015 (GtC)     /1740   /
        mateq  Equilibrium concentration atmosphere  (GtC)          /588    /
        mueq   Equilibrium concentration in upper strata (GtC)      /360    /
        mleq   Equilibrium concentration in lower strata (GtC)      /1720   /
* Flow paramaters
        b12      Carbon cycle transition matrix                     /.12   /
        b23      Carbon cycle transition matrix                     /0.007 /
* These are for declaration and are defined later
        b11      Carbon cycle transition matrix
        b21      Carbon cycle transition matrix
        b22      Carbon cycle transition matrix
        b32      Carbon cycle transition matrix
        b33      Carbon cycle transition matrix
$offtext
        mperm0 Initial stock in fastes carbon box (GtC)             /139.1 /
        mslow0 Initial stock in fastes carbon box (GtC)             /90.2  /
        mmedium0 Initial stock in fastes carbon box (GtC)           /29.2  /
        mfast0 Initial stock in fastes carbon box (GtC)             /4.2   /
        b10      proportion of emissions in permanent box           /.217   /
        b11      proportion of emissions in slowes box              /.224   /
        b12      proportion of emissions in medium box              /.282   /
        b13      proportion of emissions in fast box                /.276   /
        b21      Decay speed slowest box                            /.00254 /
        b22      Decay speed medium box                             /.0274  /
        b23      Decay speed fast box                               /.232342 /
** The following three parameters are needed for positive feedback.
        R0       pre-industrial iIRF                                / 34.4   /
```

```
        RC       iIRF response to CACC(GtC)                          / 0.019  /
        RT       iIRF response to T(°C)                              / 4.165  /
** End of changes.
        sig0     Carbon intensity 2010 (kgCO2 per output 2005 USD 2010)
** Climate model parameters
        t2xco2   Equilibrium temp impact (oC per doubling CO2)    / 3.1  /
        fex0     2015 forcings of non-CO2 GHG (Wm-2)              / 0.5  /
        fex1     2100 forcings of non-CO2 GHG (Wm-2)              / 1.0  /
        tocean0  Initial lower stratum temp change (C from 1900)  /.0068 /
        tatm0    Initial atmospheric temp change (C from 1900)    /0.85  /
        c1       Climate equation coefficient for upper level     /0.1005  /
        c3       Transfer coefficient upper to lower stratum      /0.088   /
        c4       Transfer coefficient for lower level             /0.025   /
        fco22x   Forcings of equilibrium CO2 doubling (Wm-2)      /3.6813  /
** Climate damage parameters
        a10       Initial damage intercept                         /0       /
        a20       Initial damage quadratic term
        a1        Damage intercept                                 /0       /
        a2        Damage quadratic term                            /0.00236 /
        a3        Damage exponent                                  /2.00    /
** Abatement cost
        expcost2  Exponent of control cost function               / 2.6  /
        pback     Cost of backstop 2010$ per tCO2 2015            / 550  /
        gback     Initial cost decline backstop cost per period   / .025 /
        limmiu    Upper limit on control rate after 2150          / 1.2 /
        tnopol    Period before which no emissions controls base  / 45   /
        cprice0   Initial base carbon price (2010$ per tCO2)      / 2    /
        gcprice   Growth rate of base carbon price per year       /.02   /

** Scaling and inessential parameters
* Note that these are unnecessary for the calculations
* They ensure that MU of first period's consumption =1 and PV cons = PV utilty
        scale1      Multiplicative scaling coefficient           /0.0302455265681763 /
        scale2      Additive scaling coefficient                /-10993.704/ ;

* Program control variables
sets     tfirst(t), tlast(t), tearly(t), tlate(t);

PARAMETERS
        l(t)          Level of population and labor
        al(t)         Level of total factor productivity
        sigma(t)      CO2-equivalent-emissions output ratio
        rr(t)         Average utility social discount rate
        ga(t)         Growth rate of productivity from
        forcoth(t)    Exogenous forcing for other greenhouse gases
        gl(t)         Growth rate of labor
        gcost1        Growth of cost factor
        gsig(t)       Change in sigma (cumulative improvement of energy efficiency)
        etree(t)      Emissions from deforestation
        cumetree(t)   Cumulative from land
        cost1(t)      Adjusted cost for backstop
        lam           Climate model parameter
        gfacpop(t)    Growth factor population
        pbacktime(t)  Backstop price
        optlrsav      Optimal long-run savings rate used for transversality
        scc(t)        Social cost of carbon
        cpricebase(t) Carbon price in base case
        photel(t)     Carbon Price under no damages (Hotelling rent condition)
        ppm(t)        Atmospheric concentrations parts per million
        atfrac(t)     Atmospheric share since 1850
        atfrac2010(t)     Atmospheric share since 2010 ;
* Program control definitions
        tfirst(t) = yes$(t.val eq 1);
        tlast(t)  = yes$(t.val eq card(t));
* Parameters for long-run consistency of carbon cycle
** These calculations specify DICE's transition matrix in carbon cycle. They are not needed
anymore.
$ontext
        b11 = 1 - b12;
        b21 = b12*MATEQ/MUEQ;
        b22 = 1 - b21 - b23;
        b32 = b23*mueq/mleq;
        b33 = 1 - b32 ;
$offtext
** End of changes
* Further definitions of parameters
        a20 = a2;
        sig0 = e0/(q0*(1-miu0));
```

```
        lam = fco22x/ t2xco2;
        l("1") = pop0;
        loop(t, l(t+1)=l(t););
        loop(t, l(t+1)=l(t)*(popasym/L(t))**popadj ;);

        ga(t)=ga0*exp(-dela*5*((t.val-1)));
        al("1") = a0; loop(t, al(t+1)=al(t)/((1-ga(t))););
        gsig("1")=gsigma1; loop(t,gsig(t+1)=gsig(t)*((1+dsig)**tstep) ;);
        sigma("1")=sig0;   loop(t,sigma(t+1)=(sigma(t)*exp(gsig(t)*tstep)););

        pbacktime(t)=pback*(1-gback)**(t.val-1);
        cost1(t) = pbacktime(t)*sigma(t)/expcost2/1000;

        etree(t) = eland0*(1-deland)**(t.val-1);
        cumetree("1")= 100; loop(t,cumetree(t+1)=cumetree(t)+etree(t)*(5/3.666););

        rr(t) = 1/((1+prstp_pub)**(tstep*(t.val-1)));
        forcoth(t) = fex0+ (1/17)*(fex1-fex0)*(t.val-1)$(t.val lt 18)+ (fex1-fex0)$(t.val ge
18);
        optlrsav = (dk + .004)/(dk + .004*elasmu + prstp)*gama;

*Base Case Carbon Price
        cpricebase(t)= cprice0*(1+gcprice)**(5*(t.val-1));

VARIABLES
        MIU(t)          Emission control rate GHGs
        FORC(t)         Increase in radiative forcing (watts per m2 from 1900)
        TATM(t)         Increase temperature of atmosphere (degrees C from 1900)
        TOCEAN(t)       Increase temperatureof lower oceans (degrees C from 1900)
        MAT(t)          Carbon concentration increase in atmosphere (GtC from 1750)
** Old variables are moved and new ones introduced below
$ontext
        MU(t)           Carbon concentration increase in shallow oceans (GtC from 1750)
        ML(t)           Carbon concentration increase in lower oceans (GtC from 1750)
$offtext
        MPERM(t)        Carbon concentration increase in permanent box (GtC from 1750)
        MSLOW(t)        Carbon concentration increase in slow decay box (GtC from 1750)
        MMEDIUM(t)      Carbon concentration increase in medium decay box (GtC from 1750)
        MFAST(t)        Carbon concentration increase in fast decay box (GtC from 1750)
        CACC(t)         Carbon accumulated minus past satiation (GtC)
        iIRF(T)         100-year integrated impulse response function
        alpha(T)        time constant scaling factor (positive feed-back from emissions to
reduced carbon decay)
** End of changes
        E(t)            Total CO2 emissions (GtCO2 per year)
        EIND(t)         Industrial emissions (GtCO2 per year)
        C(t)            Consumption (trillions 2005 US dollars per year)
        K(t)            Capital stock (trillions 2005 US dollars)
        CPC(t)          Per capita consumption (thousands 2005 USD per year)
        I(t)            Investment (trillions 2005 USD per year)
        S(t)            Gross savings rate as fraction of gross world product
        RI(t)           Real interest rate (per annum)
        Y(t)            Gross world product net of abatement and damages (trillions 2005 USD per
year)
        YGROSS(t)       Gross world product GROSS of abatement and damages (trillions 2005 USD
per year)
        YNET(t)         Output net of damages equation (trillions 2005 USD per year)
        DAMAGES(t)      Damages (trillions 2005 USD per year)
        DAMFRAC(t)      Damages as fraction of gross output
        ABATECOST(t)    Cost of emissions reductions  (trillions 2005 USD per year)
        MCABATE(t)      Marginal cost of abatement (2005$ per ton CO2)
        CCA(t)          Cumulative industrial carbon emissions (GTC)
        CCATOT(t)       Total carbon emissions (GtC)
        PERIODU(t)      One period utility function
        CPRICE(t)       Carbon price (2005$ per ton of CO2)
        CEMUTOTPER(t)   Period utility
        UTILITY         Welfare function;

** Obsolete variables MU and ML have been removed in the declaration of non-negative variables
below. Additional ones are introduced to reflect new carbon dynamics.
* NONNEGATIVE VARIABLES  MIU, TATM, MAT, MU, ML, Y, YGROSS, C, K, I;
NONNEGATIVE VARIABLES  MIU, TATM, MAT, Y, YGROSS, C, K, I;
NONNEGATIVE VARIABLES  MPERM, MSLOW, MMEDIUM, MFAST, alpha;

EQUATIONS
*Emissions and Damages
        EEQ(t)           Emissions equation
        EINDEQ(t)        Industrial emissions
```

```
        CCACCA(t)        Cumulative industrial carbon emissions
        CCATOTEQ(t)        Cumulative total carbon emissions
        FORCE(t)         Radiative forcing equation
        DAMFRACEQ(t)     Equation for damage fraction
        DAMEQ(t)         Damage equation
        ABATEEQ(t)       Cost of emissions reductions equation
        MCABATEEQ(t)     Equation for MC abatement
        CARBPRICEEQ(t)   Carbon price equation from abatement

*Climate and carbon cycle
        MMAT(t)          Atmospheric concentration equation
** Old carbon cycle equations are removed and new equations for carbon boxes and accounting for
past sink satiation introduced.
$ontext
        MMU(t)           Shallow ocean concentration
        MML(t)           Lower ocean concentration
$offtext
        MMPERM(t)        Permanent carbon box
        MMSLOW(t)        Slow decay carbon box
        MMMEDIUM(t)      Medium decay speed carbon box
        MMFAST(t)        Fast decay carbon box
        CACCEQ(t)        Cumulative carbon emissions(t)
        iIRFeq1(t)       calibraton of IRF to 100 year impulse
        iIRFeq2(t)
** End of changes
        TATMEQ(t)        Temperature-climate equation for atmosphere
        TOCEANEQ(t)      Temperature-climate equation for lower oceans

*Economic variables
        YGROSSEQ(t)      Output gross equation
        YNETEQ(t)        Output net of damages equation
        YY(t)            Output net equation
        CC(t)            Consumption equation
        CPCE(t)          Per capita consumption definition
        SEQ(t)           Savings rate equation
        KK(t)            Capital balance equation
        RIEQ(t)          Interest rate equation

* Utility
        CEMUTOTPEREQ(t)  Period utility
        PERIODUEQ(t)     Instantaneous utility function equation
        UTIL             Objective function      ;

** Equations of the model
*Emissions and Damages
 eeq(t)..              E(t)           =E= EIND(t) + etree(t);
 eindeq(t)..           EIND(t)        =E= sigma(t) * YGROSS(t) * (1-(MIU(t)));
 ccacca(t+1)..         CCA(t+1)       =E= CCA(t)+ EIND(t)*5/3.666;
 ccatoteq(t)..         CCATOT(t)      =E= CCA(t)+cumetree(t);
 force(t)..            FORC(t)        =E= fco22x * ((log((MAT(t)/588.000))/log(2))) + forcoth(t);
 damfraceq(t) ..       DAMFRAC(t)     =E= (a1*TATM(t))+(a2*TATM(t)**a3) ;
 dameq(t)..            DAMAGES(t)     =E= YGROSS(t) * DAMFRAC(t);
 abateeq(t)..          ABATECOST(t)   =E= YGROSS(t) * cost1(t) * (MIU(t)**expcost2);
 mcabateeq(t)..        MCABATE(t)     =E= pbacktime(t) * MIU(t)**(expcost2-1);
 carbpriceeq(t)..      CPRICE(t)      =E= pbacktime(t) * (MIU(t))**(expcost2-1);

*Climate and carbon cycle
** New carbon cycle removes old equations and introduces new equations for carbon boxes,
cumulative emissions, and saturation of sinks
$ontext
 mmat(t+1)..           MAT(t+1)       =E= MAT(t)*b11 + MU(t)*b21 + (E(t)*(5/3.666));
 mml(t+1)..            ML(t+1)        =E= ML(t)*b33  + MU(t)*b23;
 mmu(t+1)..            MU(t+1)        =E= MAT(t)*b12 + MU(t)*b22 + ML(t)*b32;
$offtext
 mmat(t)..             MAT(t)         =E= MPERM(t) + MSLOW(t) + MMEDIUM(t) +  MFAST(t) + 588  ;
 mmperm(t+1)..         MPERM(t+1)     =E= b10*5/3.666 * E(t) + MPERM(t) ;
 mmslow(t+1)..         MSLOW(t+1)     =E= b11/(b21/alpha(t)) *(1-exp(-b21/alpha(t)*5))/3.666 *
E(t) + exp(-b21/alpha(t)*5)*MSLOW(t) ;
 mmmedium(t+1)..       MMEDIUM(t+1)   =E= b12/(b22/alpha(t)) *(1-exp(-b22/alpha(t)*5))/3.666 *
E(t) + exp(-b22/alpha(t)*5)*MMEDIUM(t) ;
 mmfast(t+1)..         MFAST(t+1)     =E= b13/(b23/alpha(t)) *(1-exp(-b23/alpha(t)*5))/3.666 *
E(t) + exp(-b23/alpha(t)*5)*MFAST(t) ;
 cacceq(t)..           CACC(t)        =E= CCA(t) + cumetree(t) - (MAT(T) - 588) ;
 iIRFeq1(T)..          iIRF(T)        =E= R0 + RC*CACC(T) + RT*TATM(T) ;
 iIRFeq2(T)..          iIRF(T)        =E= b10 * 100 + alpha(t) * (
                                         + b11 / b21 * ( 1 - exp( -100*b21/alpha(t) ) )
                                         + b12 / b22 * ( 1 - exp( -100*b22/alpha(t) ) )
                                         + b13 / b23 * ( 1 - exp( -100*b23/alpha(t) ) )   );
```

```
** End of changes
 tatmeq(t+1)..        TATM(t+1)      =E= TATM(t) + c1 * ((FORC(t+1)-(fco22x/t2xco2)*TATM(t))-
(c3*(TATM(t)-TOCEAN(t))));
 toceaneq(t+1)..      TOCEAN(t+1)    =E= TOCEAN(t) + c4*(TATM(t)-TOCEAN(t));

*Economic variables
 ygrosseq(t)..        YGROSS(t)      =E= (al(t)*(L(t)/1000)**(1-GAMA))*(K(t)**GAMA);
 yneteq(t)..          YNET(t)        =E= YGROSS(t)*(1-damfrac(t));
 yy(t)..              Y(t)           =E= YNET(t) - ABATECOST(t);
 cc(t)..              C(t)           =E= Y(t) - I(t);
 cpce(t)..            CPC(t)         =E= 1000 * C(t) / L(t);
 seq(t)..             I(t)           =E= S(t) * Y(t);
 kk(t+1)..            K(t+1)         =L= (1-dk)**tstep * K(t) + tstep * I(t);
 rieq(t+1)..          RI(t)          =E= (1+prstp_pub) * (CPC(t+1)/CPC(t))**(elasmu_pub/tstep) -
1;

*Utility
 cemutotpereq(t)..    CEMUTOTPER(t)  =E= PERIODU(t) * L(t) * rr(t);
 periodueq(t)..       PERIODU(t)     =E= ((C(T)*1000/L(T))**(1-elasmu_pub)-1)/(1-elasmu_pub)-1;
 util..               UTILITY        =E= tstep * scale1 * sum(t,  CEMUTOTPER(t)) + scale2 ;

*Resource limit
CCA.up(t)       = fosslim;

* Control rate limits
MIU.up(t)             = limmiu;
MIU.up(t)$(t.val<30) = 1;

**  Upper and lower bounds for stability
K.LO(t)         = 1;
MAT.LO(t)       = 10;
** following two bounds are obsolete
*MU.LO(t)        = 100;
*ML.LO(t)        = 1000;
C.LO(t)         = 2;
TOCEAN.UP(t)    = 20;
TOCEAN.LO(t)    = -1;
TATM.UP(t)      = 20;
CPC.LO(t)       = .01;
TATM.UP(t)      = 12;

* Control variables
set lag10(t) ;
lag10(t) =  yes$(t.val gt card(t)-10);
S.FX(lag10(t)) = optlrsav;

* Initial conditions
CCA.FX(tfirst)    = 400;
K.FX(tfirst)      = k0;
** following three initial conditions are obsolete and new ones introduced.
*MAT.FX(tfirst)    = mat0;
*MU.FX(tfirst)     = mu0;
*ML.FX(tfirst)     = ml0;
MPERM.FX(tfirst)    = MPERM0;
MSLOW.FX(tfirst)    = MSLOW0;
MMEDIUM.FX(tfirst)  = MMEDIUM0;
MFAST.FX(tfirst)    = MFAST0;
** End of Changes
TATM.FX(tfirst)   = tatm0;
TOCEAN.FX(tfirst) = tocean0;

** Solution options
option iterlim = 99900;
option reslim = 99999;
option solprint = on;
option limrow = 0;
option limcol = 0;
model  CO2 /all/;

** Variables changed to match thermal warming of Geoffroy et al.
c1  = 0.386 ;
lam = 1.13  ;
c3  = 0.73  ;
c4  = 0.034 ;
fco22x = 3.503;
alpha.lo(t) = .1;
alpha.up(t) = 1000;
** Exogenous forcing components (variables etree and forcoth) are adapted to SSP1 2.6.
```

```
Parameter etree_DICE, forcoth_DICE;
etree_DICE(T)  = etree(T);
forcoth_DICE(T)= forcoth(T);
Parameter etree_SSP1_26, forcoth_SSP1_26;

forcoth_SSP1_26(T)              =  0.297 ;
forcoth_SSP1_26(T)$(T.val GE 2) =  0.393 ;
forcoth_SSP1_26(T)$(T.val GE 4) =  0.497 ;
forcoth_SSP1_26(T)$(T.val GE 6) =  0.468 ;
forcoth_SSP1_26(T)$(T.val GE 8) =  0.402 ;
forcoth_SSP1_26(T)$(T.val GE 10)=  0.342 ;
forcoth_SSP1_26(T)$(T.val GE 12)=  0.302 ;
forcoth_SSP1_26(T)$(T.val GE 14)=  0.274 ;
forcoth_SSP1_26(T)$(T.val GE 16)=  0.255 ;
forcoth_SSP1_26(T)$(T.val GE 18)=  0.257 ;

etree_SSP1_26(T)              =  3517.440/1000;
etree_SSP1_26(T)$(T.val GE 2) =  3178.329/1000;
etree_SSP1_26(T)$(T.val GE 4) =   188.063/1000;
etree_SSP1_26(T)$(T.val GE 6) = - 387.799/1000;
etree_SSP1_26(T)$(T.val GE 8) = -1758.623/1000;
etree_SSP1_26(T)$(T.val GE 10)= -2586.615/1000;
etree_SSP1_26(T)$(T.val GE 12)= -2583.968/1000;
etree_SSP1_26(T)$(T.val GE 14)= -2436.902/1000;
etree_SSP1_26(T)$(T.val GE 16)= -2084.681/1000;
etree_SSP1_26(T)$(T.val GE 18)= -2899.036/1000;

display etree_DICE, etree_SSP1_26, forcoth_DICE, forcoth_SSP1_26;
etree(T) = etree_SSP1_26(T);
forcoth(T) = forcoth_SSP1_26(T);
** End of changes

* For base run, this subroutine calculates Hotelling rents
* Carbon price is maximum of Hotelling rent or baseline price
* The cprice equation is different from 2013R. Not sure what went wrong.
If (ifopt eq 0,
       a2 = 0;
       solve CO2 maximizing UTILITY using nlp;
       photel(t)=cprice.l(t);
       a2 = a20;
);

cprice.up(t)$(ifopt=0 and t.val<tnopol+1) = max(photel(t),cpricebase(t));
miu.fx('1')$(ifopt=1 and ifmiulim=1) = miu0;
miu.lo('1')$(ifmiulim=0) = 0;
miu.up('1')$(ifmiulim=0) = 1;

solve co2 maximizing utility using nlp;
solve co2 maximizing utility using nlp;
solve co2 maximizing utility using nlp;

cprice.up(t) = inf;
miu.lo(t) = 0;
miu.up(t)            = limmiu;
miu.up(t)$(t.val<30) = 1;

** POST-SOLVE
** Output reported has been removed.

** Optimal Solution
ifopt = 1;
cprice.up(t)$(ifopt=0 and t.val<tnopol+1) = max(photel(t),cpricebase(t));
miu.fx('1')$(ifopt=1 and ifmiulim=1) = miu0;
miu.lo('1')$(ifmiulim=0) = 0;
miu.up('1')$(ifmiulim=0) = 1;
solve co2 maximizing utility using nlp;
solve co2 maximizing utility using nlp;
solve co2 maximizing utility using nlp;
cprice.up(t) = inf;

** 2°C target
TATM.up(T) = 2;
TATM.FX(tfirst)   = tatm0;
solve co2 maximizing utility using nlp;
solve co2 maximizing utility using nlp;
solve co2 maximizing utility using nlp;
TATM.up(T) = 12;
TATM.FX(tfirst)   = tatm0;
```

```
** 2°C Target without any climate damage
ifopt = 1;
TATM.up(T) = 2;
TATM.FX(tfirst)   = tatm0;
a2 = 0;
solve co2 maximizing utility using nlp;
solve co2 maximizing utility using nlp;
solve co2 maximizing utility using nlp;
a2 = a20;
TATM.up(T) = 12;
TATM.FX(tfirst)   = tatm0;
```

E Warming as a function of cumulative CO_2 emissions

Here we compare the multi-model mean response of the CMIP5 climate science models to the IAMs, scrutinising the relationship between warming and cumulative CO_2 emissions. All the models are fed with emissions from the IPCC RCP scenarios, including both CO_2 and other greenhouse gases and forcing agents. The CMIP5 multi-model mean response is obtained from Stocker et al. (2013). The CMIP5 response is quasi-linear. By contrast, most of the IAMs produce a convex response, with warming increasing more than proportionately as a function of cumulative CO_2 emissions, except for the high emissions RCP8.5 scenario and except for the Golosov et al. (2014) model. FAIR is a reasonably close approximation of the complex CMIP5 models.

Figure 11: Warming in response to cumulative CO_2 emissions, comparing the CMIP5 multi-model mean with DICE 2016

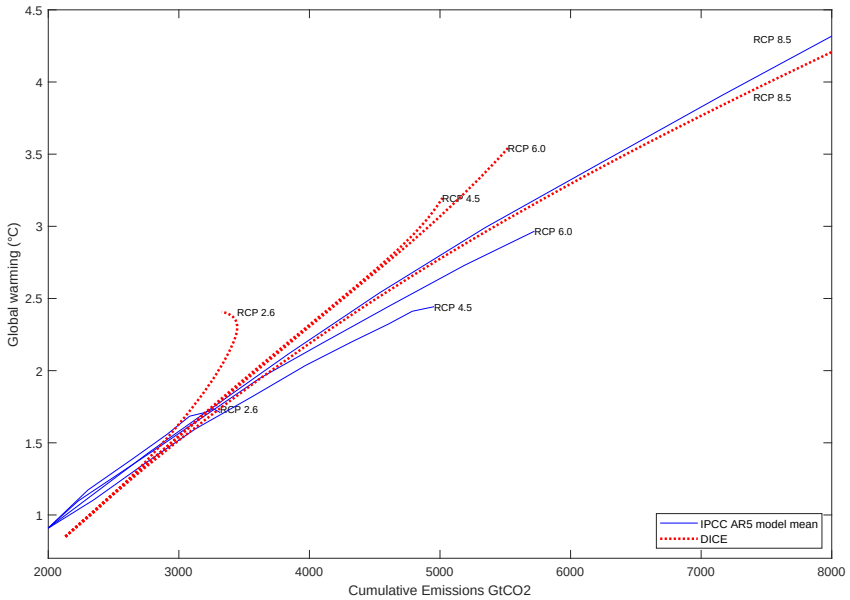

Figure 12: Warming in response to cumulative CO_2 emissions, comparing the CMIP5 multi-model mean with FUND

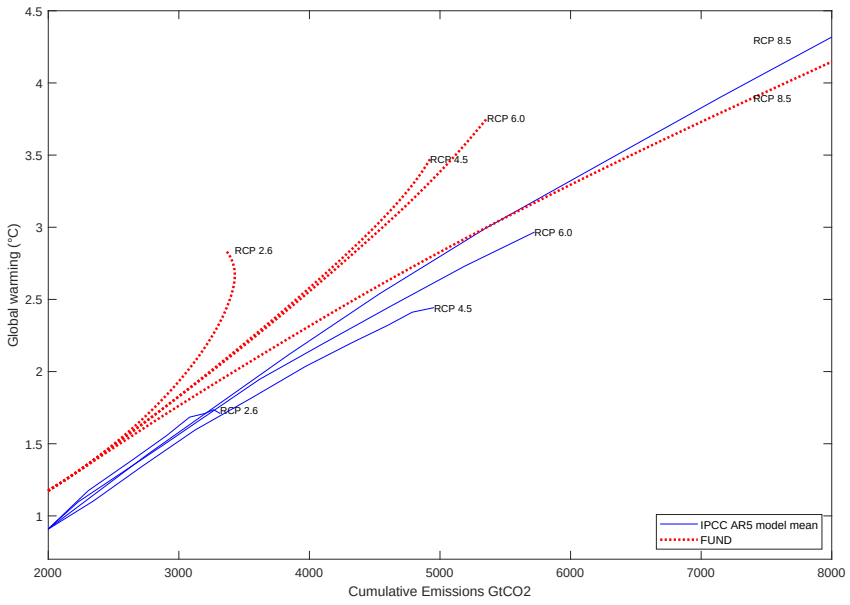

Figure 13: Warming in response to cumulative CO_2 emissions, comparing the CMIP5 multi-model mean with PAGE

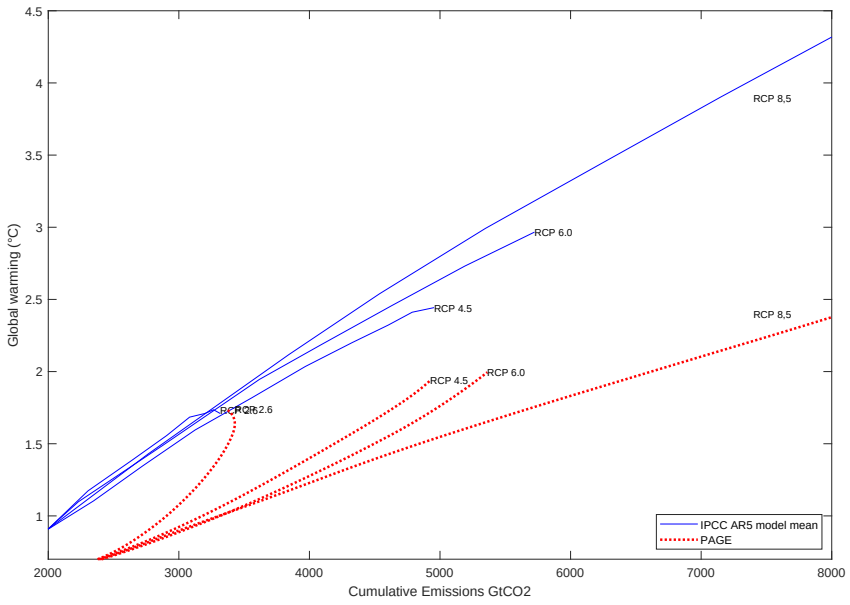

Figure 14: Warming in response to cumulative CO_2 emissions, comparing the CMIP5 multi-model mean with Golosov et al. (2014)

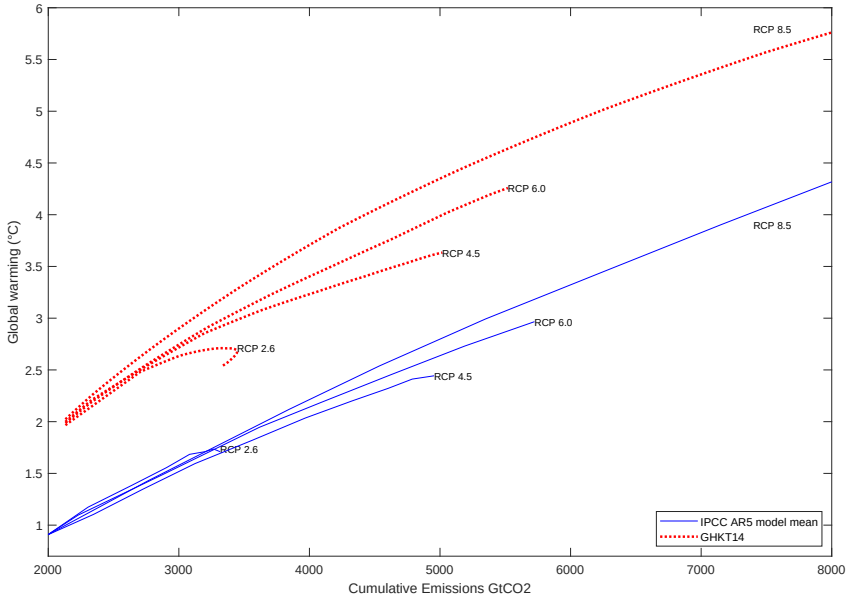

Figure 15: Warming in response to cumulative CO_2 emissions, comparing the CMIP5 multi-model mean with Gerlagh and Liski (2018)

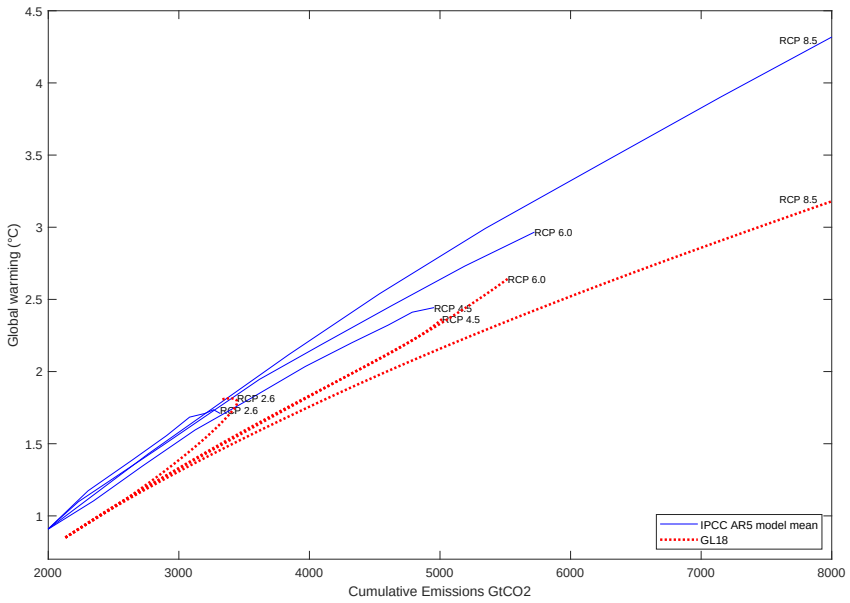

Figure 16: Warming in response to cumulative CO_2 emissions, comparing the CMIP5 multi-model mean with Lemoine and Rudik (2017)

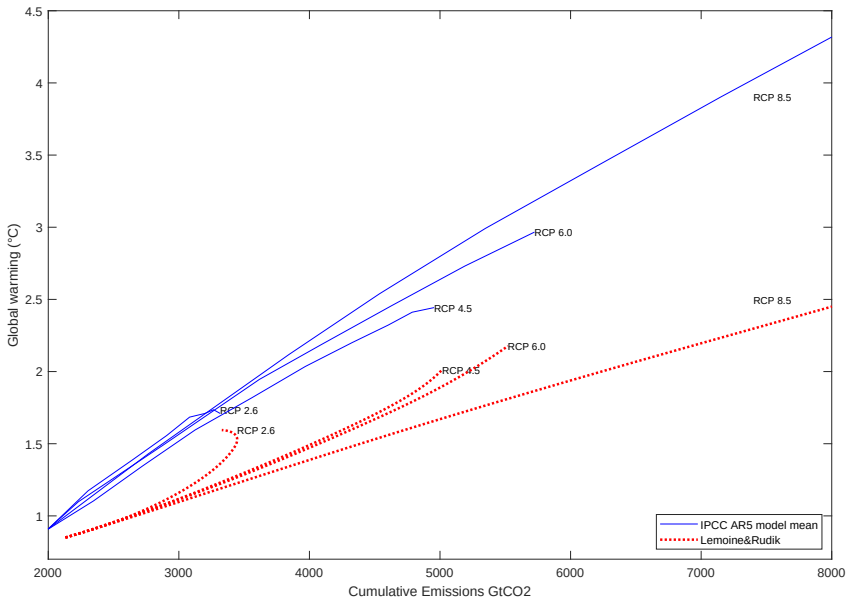

Figure 17: Warming in response to cumulative CO_2 emissions, comparing the CMIP5 multi-model mean with FAIR